

Synchronization of Chaos and Its Applications

Deniz Eroglu^{a,b}, Jeroen S.W. Lamb^b and Tiago Pereira^{a*}

^a *Instituto de Ciências Matemáticas e Computação, Universidade de São Paulo, São Carlos, Brazil;*

^b *Department of Mathematics, Imperial College London, London, UK*

(March 22, 2017)

Dynamical networks are important models for the behaviour of complex systems, modelling physical, biological and societal systems, including the brain, food webs, epidemic disease in populations, power grids and many other. Such dynamical networks can exhibit behaviour in which deterministic chaos, exhibiting unpredictability and disorder, coexists with synchronization, a classical paradigm of order. We survey the main theory behind complete, generalized and phase synchronization phenomena in simple as well as complex networks and discuss applications to secure communications, parameter estimation and the anticipation of chaos.

Keywords: synchronization; interaction; networks; stability; coupled systems

Contents

1	1 Introduction	3
2	2 Synchronization between two coupled systems	4
2.1	2.1 Synchronization of linear systems	4
2.2	2.2 Complete synchronization of nonlinear systems	6
2.2.1	2.2.1 CS in driven systems	11
2.3	2.3 Phase synchronization	12
2.4	2.4 Generalized synchronization	15
2.4.1	2.4.1 Generalized Synchronization between diffusively coupled oscillators	16
2.5	2.5 Summary of Synchronization types	18
2.6	2.6 Historical Notes	20
3	3 Applications	21
3.1	3.1 Secure Communication Based on Complete Synchronization	21
3.2	3.2 Secure Communication Based on Phase Synchronization	23
3.3	3.3 Parameter Estimation and Prediction	25
3.4	3.4 Chaos Anticipation	27
4	4 Synchronization in complex networks	29
4.1	4.1 Interactions in terms of Laplacian	31
4.2	4.2 Relation to other types of Synchronization	32
4.3	4.3 Complex Networks	32
4.4	4.4 Spectral Properties of the Laplacian	37
5	5 Stability of Synchronized Solutions	37

*Corresponding author. Email: tiago@icmc.usp.br

35	5.1	Which networks synchronize best	39
36	5.2	Proof of the Stable Synchronization	40
37	6	General Diffusive Coupling and Master Stability Function	43
38	6.1	Examples of Master Stability Functions	45
39	6.2	Synchronization conditions and Synchronization Loss	45
40	6.2.1	Extensions	46
41	7	Conclusions	48
42	A	List of frequently used notions and abbreviations	50
43	B	Lyapunov exponent	50
44	C	Lyapunov Function	51
45	D	Chaos in Lorenz system	52
46	E	Mathematical Structure of Generalized Synchronization	53

47 **1. Introduction**

48 This survey provides an introduction to the phenomenon of synchronization in coupled chaotic dynamical
 49 systems. Both chaos and synchronization are important concepts in science, from a philosophical as well
 50 as a practical point of view.

51 Synchronization expresses a notion of strong correlations between coupled systems. In its most ele-
 52 mentary and intuitive form, synchronization refers to the tendency to have the same dynamical behaviour.
 53 Scientists also recognize weaker forms of synchronization, where some key aspects of dynamical behaviour
 54 are the same - like frequencies - or where coupled dynamical behaviours satisfy a specific spatiotemporal
 55 relationship - like a constant phase lag.

56 Synchronization is fundamental to our understanding of a wide range of natural phenomena, from cos-
 57 mology and natural rhythms like heart beating [123] and hand clapping [78] to superconductors [132].
 58 While synchronization is often beneficial, some pathologies of the brain such as Parkinson disease [44, 128]
 59 and epilepsy [39] are also related to this phenomenon. In ecology, synchronization of predators can lead to
 60 extinction [31, 32] while improving the quality of synchronized behaviour of prey can increase the odds to
 61 survive [19]. In epidemiology, synchronization in measles outbreaks can cause social catastrophes [43].

62 Synchronization is also relevant to technology. Lasers form an important example. The stability of a
 63 laser generally decreases when its power increases. A successful way to create a high-power laser system
 64 is by combining many low-power stable lasers. A key challenge is to make sure that the lasers synchronize
 65 [45, 48, 83, 135], as without synchronization destructive interference diminishes power.

66 synchronization can also cause engineering problems. A recent well-publicized example concerns the
 67 *London Millennium Bridge*, traversing the River Thames. On the opening day in 2000, the bridge attracted
 68 90,000 visitors, holding up to 2000 visitors on the bridge at the same time. Lateral motion caused by the
 69 pedestrians made the bridge lurches to one side, as a result of which the pedestrians would adjust their
 70 rhythm to keep from falling over. In turn, this led to increased oscillations of the bridge due to the synchro-
 71 nization between the bridge's oscillations and pedestrians' gait [17, 33, 124]. Eventually, the oscillations
 72 became so extensive that the bridge was closed for safety reasons. The bridge was only opened to the pub-
 73 lic again after a redesign where dampers were installed to increase energy dissipation and thereby impede
 74 synchronization between bridge and pedestrians.

75 The above examples of synchronization in coupled systems describe a spontaneous transition to order
 76 because of the interaction. Coupled systems are modelled as networks of interacting elements. We often
 77 have a detailed understanding about the dynamics of the individual uncoupled elements. For example, we
 78 have reasonably good models for individual superconducting Josephson junctions, heart cells, neurons,
 79 lasers and even pedestrians. In the systems we consider here, the coupling between elements is assumed to
 80 be built up from bilateral interactions between pairs of elements, and a network structure indicating which
 81 pairs of elements interact with each other. First, the way the individuals talk to each other. For example,
 82 in the neurons the interaction is mediated by synapses and in heart cells by electrical diffusion. Second,
 83 the linking structure describing who is influencing whom. So, it is the network structure that provides
 84 the interaction among individual elements. The collective behavior emerges from the collaboration and
 85 competition of many elements mediated by the network structure.

86 Synchronization can be effectively used to create secure communication schemes [60, 105, 120]. And
 87 it can help developing new technologies. Synchronization is also used for model calibration, that is, the
 88 synchronized regime between data and equations can reveal the parameter of the equations [86, 139].

89 Chaos in dynamics is one of the scientific revolutions of the twentieth century that has deepened our
 90 understanding of the nature of unpredictability. Initiated by Henri Poincaré in the late 19th century, the
 91 chaos revolution took off in the 1980s when computers with which chaotic dynamics can be studied and
 92 illustrated, became more widely available. Chaos normally arises when recurrent dynamical behaviour has
 93 locally dispersing characteristics, as measured by a positive Lyapunov exponent. In this review, we will not
 94 discuss any details of chaotic dynamics in detail. For a comprehensive monograph on this topic, see for
 95 instance [58].

96 At first sight it may appear that the concept of synchronization, as an expression of order, and the concept

97 of chaos, associated with disorder, could not be more distant from one another. Hence, it was quite a surprise
 98 when physicists realised that coupled chaotic systems also could spontaneously synchronize [2, 38]. Despite
 99 many years of studies into this phenomenon and its applications, many fundamental problems remain open.
 100 This survey is meant to provide a concise overview of some of the most important theoretical insights
 101 underlying our current understanding of synchronization of chaos as well as highlighting some of the many
 102 remaining challenges.

103 In this review, we will discuss the basic results for synchronization of chaotic systems. The interaction
 104 can make these systems adapt and display a complicated unpredictable dynamics while behaving in a
 105 synchronous manner. Synchronization in these systems can appear in hierarchy depending on the details of
 106 the individual elements and the network structure. We will first discuss this hierarchy in two coupled chaotic
 107 oscillators and latter generalize to complex networks. The review is organised as follows. In Section 2
 108 we discuss the synchronization scenarios between two coupled oscillators. In Section 3 we discuss such
 109 applications where the synchronization phenomenon can be used for prediction and parameter estimation.
 110 In Section 4 we discuss synchronization in complex networks.

111 2. Synchronization between two coupled systems

112 2.1. Synchronization of linear systems

113 Before touching upon more topical and interesting settings in which synchronization is observed in non-
 114 linear systems, as an introduction we consider the elementary example of synchronization between two
 115 linearly coupled linear systems. Although simple, this example bears the main ideas of the general case of
 116 synchronization between two or more nonlinearly coupled systems.

We consider two identical linear systems

$$\dot{x}_i := \frac{dx_i}{dt} = ax_i, \quad i = 1, 2$$

117 with a a non-zero constant. The solution of these linear differential equations with initial condition $x_i(0)$ is
 118 $x_i(t) = e^{at}x_i(0)$ so that the ensuing dynamics is simple and all solutions converge exponentially fast to zero
 119 if $a < 0$, or diverge to infinity if $a > 0$ unless $x(0) = 0$.

120 We now consider these linear systems coupled in the following way

$$\begin{aligned} \dot{x}_1 &= ax_1 + \alpha(x_2 - x_1) \\ \dot{x}_2 &= ax_2 + \alpha(x_1 - x_2) \end{aligned} \tag{1}$$

121 and α is called the *coupling parameter*.

In the context of this model, we speak of *Complete Synchronization (CS)* if $x_1(t)$ and $x_2(t)$ converge to each other as $t \rightarrow \infty$. In order to study this phenomenon, it is natural to consider the new variable

$$z := x_1 - x_2.$$

In terms of this variable, synchronization corresponds to the fact that $\lim_{t \rightarrow \infty} z(t) = 0$. As $\dot{z} = \dot{x}_1 - \dot{x}_2$, we find directly by substitution from Eq. (1) that

$$\dot{z} = (a - 2\alpha)z,$$

122 which has the explicit solution $z(t) = z(0)e^{(a-2\alpha)t}$. Hence, we find that $\lim_{t \rightarrow \infty} z(t) = 0$ if and only if
 123 $a - 2\alpha < 0$ (unless the initial condition is already synchronized, i.e. $z(0) = 0$). Defining the *critical coupling*

124 value α_c as

$$\alpha_c := \frac{a}{2} \tag{2}$$

125 we thus obtain synchronization if the coupling parameter exceeds the critical value: $\alpha > \alpha_c$.

126 We finally note that as the system synchronizes, the coupling term converges to zero and the solution of
 127 each of the components behaves in accordance with the underlying uncoupled linear system: to be precise,
 128 $\lim_{t \rightarrow \infty} \left(x_i(t) - \frac{x_1(0)+x_2(0)}{2} e^{at} \right) = 0$ for $i = 1, 2$. It is important to note that the sign of the parameter a here
 129 determines a difference between synchronization to the trivial equilibrium (if $a < 0$) or to an exponentially
 130 growing solution (if $a > 0$).

131 In view of later generalizations, we will go through the above analysis again, exploiting more the linear
 132 structure of the problem so that we can appreciate synchronization in terms of spectral properties of the
 133 coupling term.

134 With $\mathbf{x} := \begin{pmatrix} x_1 \\ x_2 \end{pmatrix}$, (1) can be written as

$$\dot{\mathbf{x}} = [a\mathbf{I} - \alpha\mathbf{L}]\mathbf{x} \tag{3}$$

where

$$\mathbf{I} = \begin{pmatrix} 1 & 0 \\ 0 & 1 \end{pmatrix} \text{ and } \mathbf{L} = \begin{pmatrix} 1 & -1 \\ -1 & 1 \end{pmatrix}.$$

135 \mathbf{L} is known as the *Laplacian matrix*. In Section 4, we will generalize it to any network. The solution of (3)
 136 with initial condition $\mathbf{x}(0)$ is

$$\mathbf{x}(t) = e^{[a\mathbf{I} - \alpha\mathbf{L}]t} \mathbf{x}(0), \text{ where } e^{A t} := \sum_{n=0}^{\infty} \frac{t^n}{n!} A^n. \tag{4}$$

137 To solve (4) we note that since \mathbf{I} and \mathbf{L} commute,

$$e^{[a\mathbf{I} - \alpha\mathbf{L}]t} = e^{a\mathbf{I}t} e^{-\alpha\mathbf{L}t}$$

138 and $e^{a\mathbf{I}t} = e^{at}\mathbf{I}$. In order to evaluate $e^{-\alpha\mathbf{L}t}$, it is useful to observe that $\mathbf{v}_1 = (1, 1)^*$ and $\mathbf{v}_2 = (1, -1)^*$ are the
 139 eigenvectors of \mathbf{L} for its corresponding eigenvalues $\lambda_1 = 0$ and $\lambda_2 = 2$. As $\{\mathbf{v}_1, \mathbf{v}_2\}$ is a basis of \mathbb{R}^2 , we may
 140 write any initial condition as $\mathbf{x}(0) = c_1\mathbf{v}_1 + c_2\mathbf{v}_2$ with $c_1, c_2 \in \mathbb{R}$, so that

$$e^{-\alpha\mathbf{L}t} \mathbf{x}(0) = c_1\mathbf{v}_1 + c_2e^{-\alpha\lambda_2 t} \mathbf{v}_2$$

141 and

$$\mathbf{x}(t) = e^{[a\mathbf{I} - \alpha\mathbf{L}]t} \mathbf{x}(0) = c_1e^{at} \mathbf{v}_1 + c_2e^{(a - \alpha\lambda_2)t} \mathbf{v}_2. \tag{5}$$

142 Synchronization corresponds to the phenomenon that $\mathbf{x}(t)$ converges to the *synchronization subspace* gen-
 143 erated by \mathbf{v}_1 . This only happens if $\lim_{t \rightarrow \infty} c_2e^{(a - \alpha\lambda_2)t} \mathbf{v}_2 = 0$, i.e. if $\alpha > \frac{a}{\lambda_2}$. Thus in view of (2), we define
 144 the *critical coupling* value

$$\alpha_c = \frac{a}{\lambda_2} = \frac{a}{2}.$$

145 We note that the critical coupling value is expressed in terms of the gap between the lowest eigenvalue 0
 146 and smallest nonzero (and positive) eigenvalue of the Laplacian L .

147 **2.2. Complete synchronization of nonlinear systems**

148 We now consider two fully diffusively coupled identical nonlinear n -dimensional systems

$$\begin{aligned}\dot{\mathbf{x}}_1 &= \mathbf{f}(\mathbf{x}_1) + \alpha \mathbf{H}(\mathbf{x}_2 - \mathbf{x}_1) \\ \dot{\mathbf{x}}_2 &= \mathbf{f}(\mathbf{x}_2) + \alpha \mathbf{H}(\mathbf{x}_1 - \mathbf{x}_2)\end{aligned}\tag{6}$$

149 where $\mathbf{f}: \mathbb{R}^n \rightarrow \mathbb{R}^n$ is in general nonlinear and $\mathbf{H}: \mathbb{R}^n \rightarrow \mathbb{R}^n$ is a smooth coupling function. We assume that
 150 $\mathbf{H}(\mathbf{0}) = \mathbf{0}$ so that the synchronization subspace $\mathbf{x}_1 = \mathbf{x}_2$ is invariant for all coupling strengths α . Meaning
 151 that for any synchronized initial condition the entire solution remains synchronized: as in the synchronized
 152 state the diffusive coupling term vanishes, the dynamics is identical to that of the uncoupled system (with
 153 $\alpha = 0$). Consequently, the coupling has no influence on the synchronized motion. In particular, it could be
 154 the case that the synchronized motion is chaotic, if the uncoupled systems exhibit such behaviour.

155 We aim to show that if the coupling is sufficiently strong, the system Eq. (6) will synchronize $\mathbf{x}_1(t) -$
 156 $\mathbf{x}_2(t) \rightarrow 0$ as $t \rightarrow \infty$. We consider $\mathbf{H} = \mathbf{I}$ (the identity matrix) then the term reads as

$$\alpha \mathbf{H}(\mathbf{x}_2 - \mathbf{x}_1) = \alpha(\mathbf{x}_2 - \mathbf{x}_1).$$

157 To analyze stability, we consider – as before – the evolution of the difference variable $\mathbf{z} := \mathbf{x}_1 - \mathbf{x}_2$ in
 158 terms of which the synchronization subspace is characterized as $\mathbf{z} = 0$:

$$\begin{aligned}\dot{\mathbf{z}} &= \dot{\mathbf{x}}_1 - \dot{\mathbf{x}}_2 \\ &= \mathbf{f}(\mathbf{x}_1) - \mathbf{f}(\mathbf{x}_2) - 2\alpha \mathbf{z}\end{aligned}\tag{7}$$

159 The aim is to identify sufficient conditions for the coupling parameter α to guarantee that locally near $\mathbf{z} = 0$
 160 we have $\lim_{t \rightarrow \infty} \mathbf{z}(t) = \mathbf{0}$. To this end, we linearize the equations of motion Eq. (8) near $\mathbf{z} = 0$. We note to
 161 this extent that near $\mathbf{x}_1 = \mathbf{x}_2$ we obtain by Taylor expansion that

$$\begin{aligned}\mathbf{f}(\mathbf{x}_2(t)) &= \mathbf{f}(\mathbf{x}_1(t)) - D\mathbf{f}(\mathbf{x}_1(t))(\mathbf{x}_2(t) - \mathbf{x}_1(t)) + O(\|\mathbf{x}_1(t) - \mathbf{x}_2(t)\|^2) \\ &= \mathbf{f}(\mathbf{x}_1(t)) - D\mathbf{f}(\mathbf{x}_1(t))\mathbf{z}(t) + O(\|\mathbf{z}(t)\|^2).\end{aligned}$$

162 Here $D\mathbf{f}(\mathbf{x}_1(t))$ is the derivative (Jacobian matrix of $\mathbf{f}(\mathbf{x})$) at $\mathbf{x} = \mathbf{x}_1(t)$. We use this to write Eq. (8) near
 163 $\mathbf{z} = 0$ as

$$\frac{d\mathbf{z}}{dt} = [D\mathbf{f}(\mathbf{x}_1(t)) - 2\alpha \mathbf{I}]\mathbf{z} + O(\|\mathbf{z}\|^2).\tag{9}$$

164 The linear part of this equation, obtained by ignoring the $O(\|\mathbf{z}\|^2)$ term in Eq. (9), is commonly known as the
 165 *first variational equation*. It should be noted that this equation is nonautonomous as it depends explicitly
 166 on the reference solution $\mathbf{x}_1(t)$. In general it is not easy to analyze nonautonomous differential equations,
 167 not even linear ones. Fortunately, we are able to achieve insights without solving this equation because the
 168 coupling is rather convenient adding an extra damping term $-\alpha \mathbf{z}$.

169 To simplify the analysis, we introduce a new variable

$$\mathbf{w}(t) = e^{2\alpha t} \mathbf{z}(t)\tag{10}$$

170 in terms of which the linear part of Eq. (9) becomes precisely the variational equation for the solution $\mathbf{x}_1(t)$

171 of the uncoupled equation of motion $\dot{\mathbf{x}} = \mathbf{f}(\mathbf{x})$:

$$\begin{aligned} \dot{\mathbf{w}}(t) &= 2\alpha e^{2\alpha t} \mathbf{z}(t) + e^{2\alpha t} \dot{\mathbf{z}}(t) \\ &= 2\alpha \mathbf{w} + [D\mathbf{f}(\mathbf{x}_1(t)) - 2\alpha \mathbf{I}] e^{2\alpha t} \mathbf{z} \\ &= [D\mathbf{f}(\mathbf{x}_1(t))] \mathbf{w}. \end{aligned} \tag{11}$$

172 Let $\Phi(\mathbf{x}_1(t))$ be the fundamental matrix for the variational equation, so that any solution of this nonau-
 173 tonomous equation can be written as $\mathbf{z}(t) = \Phi(\mathbf{x}_1(t))\mathbf{z}(0)$. Let $\{\lambda_j(\mathbf{x}_1(t))\}_{j=1}^n$ be the set of positive square
 174 roots of the eigenvalues of the symmetric matrix $\Phi(\mathbf{x}_1(t))^* \Phi(\mathbf{x}_1(t))$ (where $*$ denotes transpose). Then we
 175 define

$$\Lambda := \max_j \lim_{t \rightarrow \infty} \frac{1}{t} \lambda_j(\mathbf{x}_1(t)). \tag{12}$$

176 Λ is known as the *Lyapunov exponent* of the orbit $\mathbf{x}_1(t)$ and it measures the infinitesimal asymptotic diver-
 177 gence rate near this trajectory. We refer to Appendix B for more details about the Lyapunov exponent.

178 The assertion now is that if the orbit $\mathbf{x}_1(t)$ has Lyapunov exponent Λ , then there exists a constant $C > 0$
 179 such that

$$\|\mathbf{w}(t)\| \leq C e^{\Lambda t}. \tag{13}$$

From Eq. (13) and using Eq.(10) we obtain that

$$\|\mathbf{z}(t)\| \leq C e^{(\Lambda - 2\alpha)t}.$$

Hence,

$$\alpha_c := \frac{\Lambda}{2}$$

180 is a critical coupling strength for synchronization, above which observe synchronization.

181 A complication with the above analysis, is that the Lyapunov exponent Λ and constant C may depend
 182 on the chosen trajectory $\mathbf{x}_1(t)$. The probabilistic (ergodic) theory of dynamical systems, which we will not
 183 dwell on here, asserts that often the Lyapunov exponent is constant for almost all trajectories on a given at-
 184 tractor. However, the constant C may still vary per trajectory, which leads to *non-uniform* synchronization,
 185 implying the potential of large variation of transit times until synchronization occurs. For similar phenom-
 186 ena, see also [7, 8]. We now proceed to apply the above to the examples of coupled Lorenz and Rössler
 187 systems.

188 **Lorenz system.** The Lorenz system was introduced by Edward Lorenz in 1963 as a simplified model for
 189 atmospheric convection:

$$\begin{aligned} \dot{x} &= \sigma(y - x), \\ \dot{y} &= x(\rho - z) - y, \\ \dot{z} &= -\beta z + xy, \end{aligned} \tag{14}$$

190 where the three coordinates x , y and z represent the state of the system and σ , ρ , β are parameters. When
 191 parameter values are chosen as $\sigma = 10$, $\rho = 28$ and $\beta = 8/3$, the equations display unpredictable (chaotic)
 192 dynamics. Lorenz used this choice of parameters in his original paper [66]. We use these parameter values
 193 as well.

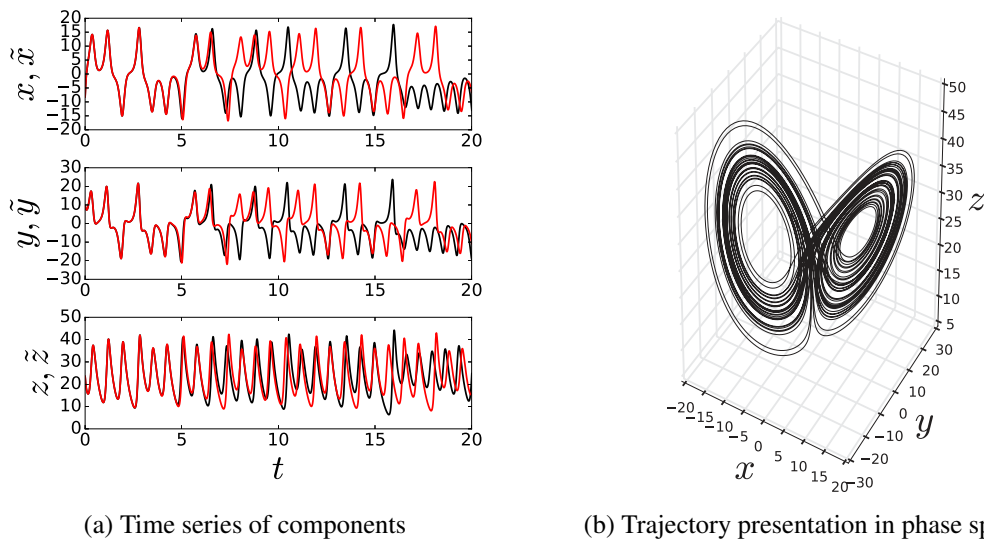


Figure 1.: Illustration of the chaotic dynamics of the Lorenz system (14) with parameter values $\sigma = 10$, $\rho = 28$ and $\beta = 8/3$. (a) Two simulations for the Lorenz system starting from two slightly different initial conditions $(x, y, z) = (-10, 10, 25)$ and $(\tilde{x}, \tilde{y}, \tilde{z}) = (-10.01, 10, 25)$. The Lorenz attractor has a positive Lyapunov exponent and the trajectories diverge from each other. (b) Representation of the trajectory of $(x, y, z) = (-10, 10, 25)$ in the phase space. The shape of the attractor resembles a butterfly.

The Lorenz equations are dissipative and all trajectories eventually enter the absorbing domain

$$\Omega = \left\{ \mathbf{x} \in \mathbb{R}^3 : \rho x^2 + \sigma y^2 + \sigma(z - 2\rho)^2 < \frac{\beta^2 \rho^2}{\beta - 1} \right\},$$

194 see Appendix C or Ref. [119]. For the classical parameters, $\sigma = 10$, $\rho = 28$ and $\beta = 8/3$, inside Ω , trajectory
 195 accumulates on the chaotic Lorenz attractor [131], as depicted in Fig. 1b. Close to the attractor nearby
 196 trajectories diverge. To see this, we simulate two trajectories with nearly the same initial condition. The
 197 initial 10^{-2} difference grows to roughly 10^2 in a matter of only six cycles, see Fig. 1a. Using numerical
 198 simulations, we estimate the maximal divergence rate of nearby trajectories $\Lambda \approx 0.906$.

199 We consider two coupled chaotic Lorenz oscillators, as in Eq. (6). We derived above that the critical
 200 coupling α_c for synchronization depends on the Lyapunov exponent Λ . Using the numerical results for Λ
 201 we obtain

$$\alpha_c = \frac{\Lambda}{2} \approx 0.453.$$

202 Simulation confirms that this critical coupling is sharp. Indeed, for $\alpha = 0.4$ there is no synchroniza-
 203 tion, and trajectories do not move together, see Fig. 2a. On the other hand, when $\alpha = 0.5$, the trajectories
 204 synchronize, see Fig. 2b).

205 To compare the amount of synchronization at different parameter values, we may consider the average
 206 deviation from synchronization during a time-interval of length T as

$$E = \frac{1}{T} \int_{t=0}^T \|\mathbf{x}_1(t) - \mathbf{x}_2(t)\| dt \quad (15)$$

207 In Fig. 3a we present a synchronization diagram where we plot E against the coupling strength α . We
 208 observe a good correspondence with the derived value of α_c . The synchronization error depends on initial
 209 conditions so that we compute the synchronization diagram via averaging over some realizations.

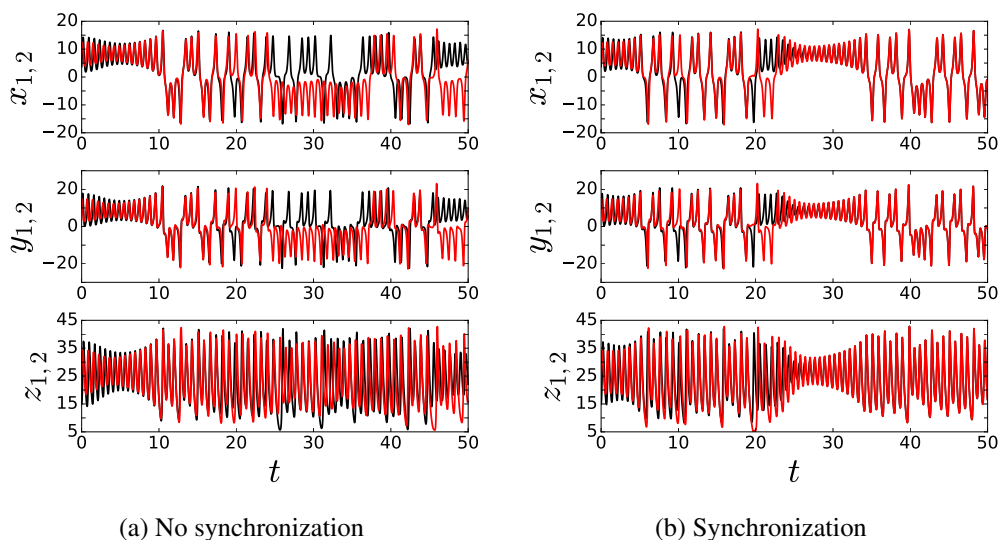


Figure 2.: Comparison of trajectories of two initial conditions for the system of two coupled Lorenz systems. The critical transition coupling is $\alpha_c \approx 0.453$ for the classical parameters. The initial conditions are selected as $(x_1, y_1, z_1) = (3, 10, 15)$ and $(x_2, y_2, z_2) = (10, 15, 25)$. (a) When $\alpha = 0.4 < \alpha_c$, there is no synchronization. (b) If $\alpha = 0.5 > \alpha_c$ one observes synchronization of trajectories.

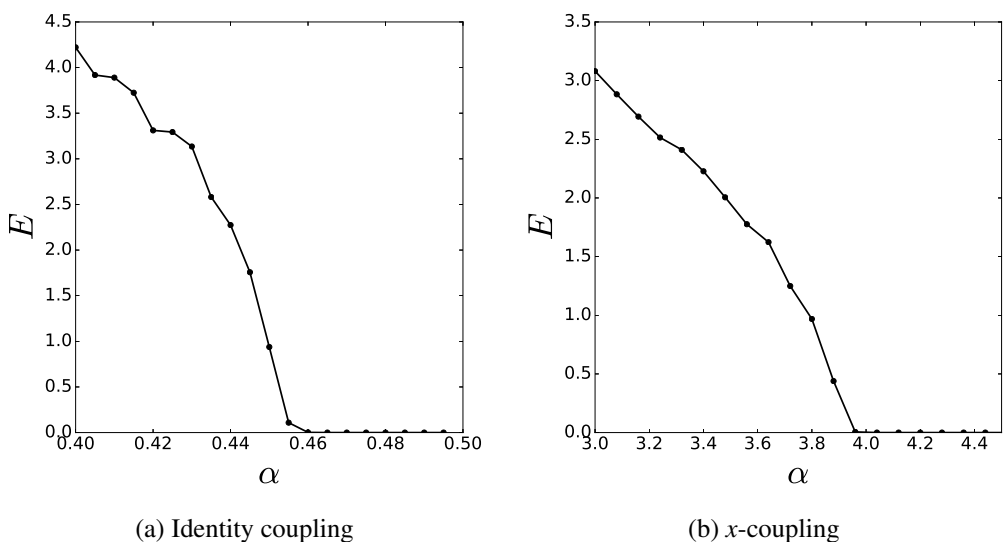


Figure 3.: Synchronization diagram of two coupled Lorenz systems, (a) with coupling matrix $\mathbf{H} = \mathbf{I}$ and (b) with coupling matrix \mathbf{H} as in Eq. (16). When $\mathbf{H} = \mathbf{I}$, the observed critical coupling constant corresponds to the theoretically derived value $\alpha_c \sim 0.453$. With coupling matrix (16), synchronisation is observed to set in for coupling strengths larger than ~ 3.75 . The synchronization error E was averaged over 300 realisations. Each realisation is simulated by a fourth order Runge-Kutta scheme for 2000 seconds with 0.01 time step.

210

211 **Examples on different coupling functions.** It is worth mentioning that this above analysis works when the
 212 coupling adds a damping term αz in other words when $\mathbf{H} = \mathbf{I}$. Indeed, the damping term in general form is
 213 $\alpha \mathbf{H} z$ and in this case the above results can no longer be applied. Therefore the synchronization depends on

214 the coupling function, we here just illustrate the effect on synchronization if \mathbf{H} is chosen to be

$$\mathbf{H} = \begin{pmatrix} 1 & 0 & 0 \\ 0 & 0 & 0 \\ 0 & 0 & 0 \end{pmatrix}, \tag{16}$$

215 implying that the coupling arises only via the first coordinate x . The corresponding synchronization diagram
 216 shows that the critical coupling α_c for x -coupling increases as a result, see Fig. 3b. Importantly, when \mathbf{H}
 217 does not commute with the Jacobian matrix along the trajectory, we cannot use the ansatz of Eq. (10). In
 218 that case we need a different approach to derive the critical coupling, which will be discussed in Section 4
 219 that deals with synchronization in complex networks.

220 **Rössler System.** As a final example, we consider a system introduced by Otto Rössler in 1976:

$$\begin{aligned} \dot{x} &= -y - z, \\ \dot{y} &= x + ay, \\ \dot{z} &= b + z(x - c), \end{aligned} \tag{17}$$

221 where a, b and c denote parameters.

222 We consider two coupled Rössler systems with identity coupling function $\mathbf{H} = \mathbf{I}$ and coupling parameter
 223 α , as in Eq. (6). We consider parameter values $a = 0.2$, $b = 0.2$ and $c = 5.7$. We numerically find that
 224 the corresponding attractor has a Lyapunov exponent $\Lambda \approx 0.071$. Hence, the expected critical coupling for
 225 synchronization is

$$\alpha_c = \frac{\Lambda}{\lambda_2} \approx 0.0355 \tag{18}$$

226 This is in excellent agreement with the numerical results is shown in the synchronization diagram Fig.4.

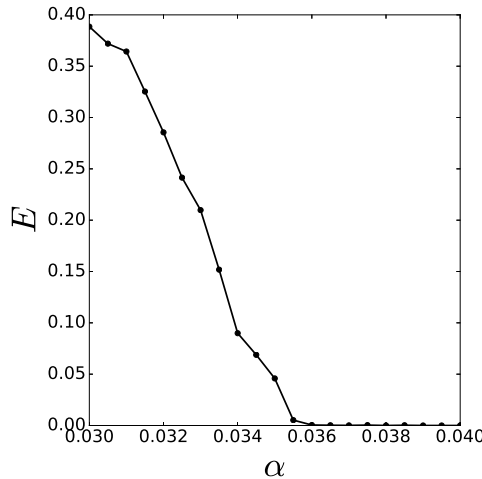


Figure 4.: The synchronization diagram of two coupled Rössler systems with the coupling function $\mathbf{H} = \mathbf{I}$. The theoretical critical coupling constant $\alpha_c \approx 0.0355$ indeed corresponds to the numerically observed one. The synchronization error E was averaged over 300 realisations. Each realisation is simulated by a fourth order Runge-Kutta scheme for 2000 seconds with 0.01 time step.

227 2.2.1. CS in driven systems

228 Another possibility is that we use certain sets of variables to drive a subsystem. For appropriate choices we
 229 can observe synchronization [89]. We illustrate this scheme in the Lorenz system where x -component can
 230 be driving signal of another identical system Fig. 5.

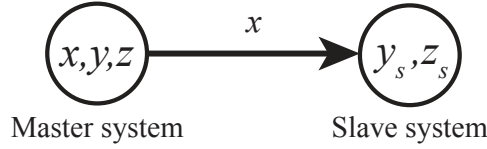


Figure 5.: Master-Slave configuration where, x -variable is made identical to the response and thereby it drives the response subsystem.

231 In this scheme we consider the variable x for the master the same as in the slave. That is, the x - variable
 232 of the master is fully replaced to the x variable in the slave

$$\begin{aligned} \dot{x} &= \sigma(y - x) \\ \dot{y} &= x(\rho - z) - y & \dot{y}_s &= x(\rho - z_s) - y_s \\ \dot{z} &= -\beta z + xy & \dot{z}_s &= -\beta z_s + xy_s \end{aligned} \tag{19}$$

233 where (x, y, z) are the states of the master system and (y_s, z_s) are the states of the slave system. In order to
 234 check the behaviour of the trajectories, we track the simultaneous variation of the trajectories by $\Delta_y(t) =$
 235 $y(t) - y_s(t)$ and $\Delta_z(t) = z(t) - z_s(t)$. For given initial conditions $(x, y, z, y_s, z_s) = (-10.1, 10.1, 10.1, 0.1, 0.1)$,
 236 Δ_y and Δ_z goes to zero (Fig. 6).

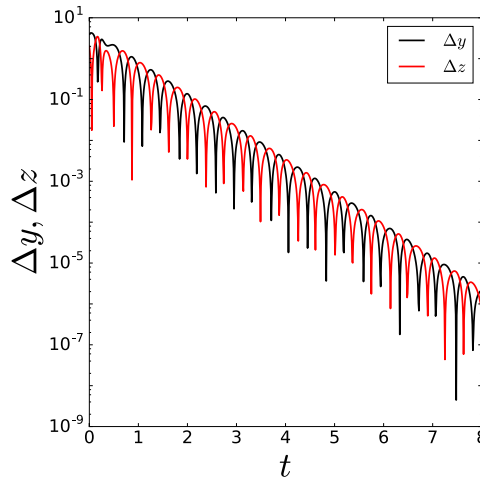


Figure 6.: Simulation of master-slave type of coupling

237 For this particular choice of subsystem it is possible to construct a Lyapunov function for the displacements $\Delta_y = y - y_s$ and $\Delta_z = z - z_s$ for x -driven system (Eq. (19)). We obtain
 238

$$\begin{aligned} \dot{\Delta}_y &= -\Delta_y - x\Delta_z \\ \dot{\Delta}_z &= x\Delta_y - \beta\Delta_z. \end{aligned} \tag{20}$$

Next consider the Lyapunov function

$$V = \frac{1}{2} (\Delta_y^2 + \Delta_z^2),$$

and along solutions of the subsystem we obtain $\dot{V} = \Delta_y \dot{\Delta}_y + \Delta_z \dot{\Delta}_z$, after some manipulation we obtain

$$\dot{V} = -\Delta_y^2 - \beta \Delta_z^2.$$

239 Since V is positive and \dot{V} negative Δ_y and Δ_z will converge to zero. So, the slave subsystem will have the
240 same dynamics as the master.

241 2.3. Phase synchronization

If there are small mismatches between the systems another type of synchronization can appear for very small coupling strengths: *Phase Synchronization* (PS) – which corresponds to a locking of phases of chaotic oscillators

$$|m\phi_1(t) - n\phi_2(t)| < C$$

242 where ϕ is the phase of the chaotic oscillators, m, n and C are constants. When this holds we have phase
243 synchronization between the two systems [108, 109]. We are considering the phases on the lift, that is,
244 diverging steadily as opposed to consider the phase mod 2π . The phase difference won't be precisely zero
245 because of the chaotic nature of the system. We could consider higher relations of phase locking, however,
246 the higher the relation $m : n$ more difficult is to observe the phase synchronization. Therefore, our examples
247 will be for 1 : 1 phase synchronization.

Phase synchronization is also vast research periodic oscillators [96, 101, 107, 129, 130]. In this case, the phases may be perfectly locked. If we are considering periodic oscillators the phase reduction approach will lead to a description of the interaction in terms of the phases alone [65]. The simplest equation in this setting is

$$\dot{\phi}_{1,2} = \omega_{1,2} + \alpha \sin(\phi_{2,1} - \phi_{1,2})$$

where ϕ is the phase along the periodic orbit. Introducing the phase difference $\Phi = \phi_1 - \phi_2$ and $\Delta = \omega_1 - \omega_2$ we obtain

$$\dot{\Phi} = \Delta - 2\alpha \sin \Phi$$

248 this equation has a stable fixed point $\Phi = \phi_1 - \phi_2 = \text{constant}$ if $\alpha > \alpha_c = |\Delta|/2$.

249 For a chaotic oscillator if coupling strength is small, the amplitudes will remain chaotic but the phase
250 difference will be bounded. Though, it will oscillate as a result of the coupling to the amplitude. In general,
251 it is not straightforward to introduce a phase for a chaotic attractor [10, 11, 56, 97, 102]. For a suitable class
252 of attractors it is possible to define a phase in a useful way.

253 We focus on coupled two nonidentical Rössler oscillators, the equation is given by

$$\begin{aligned} \dot{x}_{1,2} &= -\omega_{1,2}y_{1,2} - z_{1,2} + \alpha(x_{2,1} - x_{1,2}) \\ \dot{y}_{1,2} &= \omega_{1,2}x_{1,2} + ay_{1,2} \\ \dot{z}_{1,2} &= b + z_{1,2}(x_{1,2} - c) \end{aligned} \tag{21}$$

254 where $a = 0.165$, $b = 0.2$ and $c = 10$ are the constants of the Rössler system. ω is the mismatch parameter
255 to make the oscillators *nonidentical* and given as $\omega_{1,2} = \omega_0 \pm \Delta$ where $\omega_0 = 0.97$ and $\Delta = 0.02$. α is

256 the coupling constant, the system is coupled over x components (x -coupling). For certain values of the
 257 parameter a , the projection of the attractor on $x - y$ plane resembles a limit cycle and the trajectories rotates
 258 around the origin (see Fig. 7), and phase and amplitudes are given by

$$\phi_{1,2} = \arctan\left(\frac{y_{1,2}}{x_{1,2}}\right) \quad (22)$$

259

$$A_{1,2} = \sqrt{x_{1,2}^2 + y_{1,2}^2}. \quad (23)$$

We consider the phase on the lift (growing in time without taking the mod).

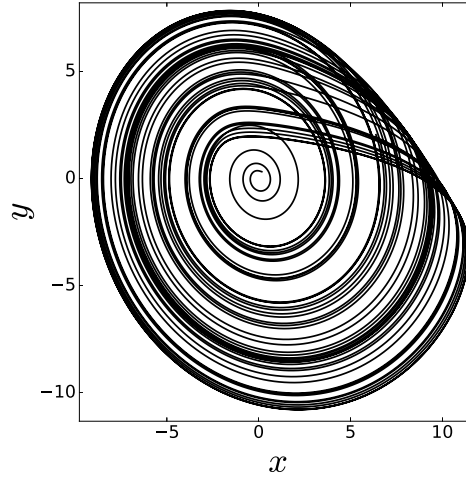


Figure 7.: Projection of the Rössler attractor on $x - y$ plane for $a = 0.165$.

260 To gain insight on the adjustment of rhythm leading to phase synchronization, we analyze the average
 261 frequencies defined as
 262

$$\Omega_{1,2} = \lim_{T \rightarrow \infty} \frac{\phi_{1,2}(T) - \phi_{1,2}(0)}{T}. \quad (24)$$

263 And the frequency mismatch is

$$\Delta\Omega = \Omega_2 - \Omega_1 \quad (25)$$

264 When phase synchronization occurs $|\phi_1(t) - \phi_2(t)| \leq C$, the average frequency is the same $\Delta\Omega = 0$. The
 265 phase difference will not be tend to a constant as the phase nature of the amplitudes acts as a noise in the
 266 phases causing mismatches. The comparison of the amplitude difference (Eq. (15)) and the phase (Eq. (25))
 267 is given in Fig. 8. If we increase the coupling constant α .

268 An approximate theory of phase synchronization can be obtained by averaging [111]. We write the model
 269 Eq. (21) in terms of the phase Eqs. (22) as

$$\dot{\phi}_{1,2} = \frac{x_{1,2}\dot{y}_{1,2} - y_{1,2}\dot{x}_{1,2}}{A^2} \quad (26)$$

270 In this form, using polar coordinates we have $x_{1,2} = A_{1,2} \cos \phi_{1,2}$ and $y_{1,2} = A_{1,2} \sin \phi_{1,2}$, and using this
 271 representation in Eq. (26), we obtain

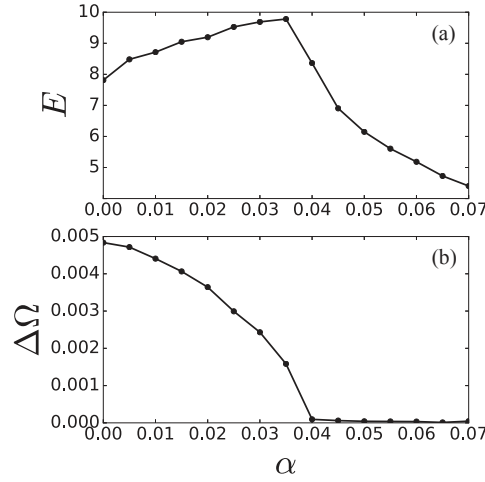


Figure 8.: For a weak coupling constant: Although there is no synchrony for the difference of the amplitudes Eq. (15)(top panel), there is a tendency towards to phase synchronization while the coupling constant α increases Eq. (24) (bottom panel). The synchronization error E and frequency mismatch $\Delta\Omega$ were averaged over 300 realisations. Each realisation is simulated by a fourth order Runge-Kutta scheme for 2000 seconds with 0.01 time step.

$$\dot{\phi}_{1,2} = \omega_{1,2} + a \sin \phi_{1,2} \cos \phi_{1,2} + \frac{z_{1,2}}{A_{1,2}} \sin \phi_{1,2} - \alpha \left(\frac{A_{2,1}}{A_{1,2}} \cos \phi_{2,1} \sin \phi_{1,2} - \cos \phi_{1,2} \sin \phi_{1,2} \right) \quad (27)$$

The idea now is that since the mismatch is small, both phases behave nearly the same. So we can split the dynamics of the phases as an overall increasing trend $\omega_0 t$ and a slow phase dynamics θ . This split is very clear in Fig. 13. So, we write

$$\phi_{1,2} = \omega_0 t + \theta_{1,2},$$

272 To obtain an equation for θ (simpler than the one for ϕ) we use the fact that θ is a slow variable. That
 273 is, while $\omega_0 t$ grows a lot θ is nearly constant. Hence, we will average out the contribution of $\omega_0 t$. So we
 274 average the phases over $\omega_0 t$ over a period $\frac{2\pi}{\omega_0}$ and keep $\theta_{1,2}$ fixed. After some laborious manipulation we
 275 obtain

$$\frac{d}{dt}(\theta_1 - \theta_2) = 2\Delta - \frac{\alpha}{2} \left(\frac{A_2}{A_1} + \frac{A_1}{A_2} \right) \sin(\theta_1 - \theta_2) \quad (28)$$

276 Both amplitudes $A_{1,2}$ depend on time and display a chaotic behaviour. Lets assume for a moment that
 277 they are constant. Then for the phase locking of the Rössler systems, $\frac{d}{dt}(\theta_1 - \theta_2) = 0$, the equation has a
 278 stable fixed point,

$$\theta_1 - \theta_2 = \arcsin \frac{4\Delta A_1 A_2}{\alpha(A_1^2 + A_2^2)}. \quad (29)$$

This fixed point only exists when the argument of the arcsin has modulus less than 1. Therefore, we obtain the critical transition coupling

$$\alpha_c \approx 2\Delta.$$

279 For the given parameters ($\Delta = 0.02$) we find $\alpha_c \approx 0.04$, in agreement with the numerical analysis Fig. 8. The
 280 chaotic behaviour of the amplitudes leads to fluctuations of the phases around the stable fixed point, and
 281 so the phases different will not be identically zero. Close to the critical coupling strength the frequencies
 282 exhibit a critical behaviour $\Delta\Omega \propto |\alpha - \alpha_c|^{1/2}$ as observed observed in Fig. 8.

283 **2.4. Generalized synchronization**

284 When the interacting systems are different, either because of a large parameter mismatch or the systems
 285 have distinct dynamics, these two can still exhibit synchronization in a generalized sense. *Generalized*
 286 *Synchronization* (GS) can be observed in mutually coupled systems as well as unidirectionally coupled
 287 system [46, 64, 89, 126]. Surprisingly, GS can be a mapped to a complete synchronization (CS) problem!

288 Here we will focus on the dynamics of unidirectionally coupled systems. The master \mathbf{x} and the slave \mathbf{y}
 289 systems coupled as

$$\begin{aligned} \dot{\mathbf{x}} &= \mathbf{f}(\mathbf{x}) \\ \dot{\mathbf{y}} &= \mathbf{g}(\mathbf{y}, \mathbf{h}(\mathbf{x})) \end{aligned} \tag{30}$$

where $\mathbf{x} \in \mathbb{R}^n$, $\mathbf{y} \in \mathbb{R}^m$ and $\mathbf{h}(\mathbf{x})$ is the coupling. For certain coupling strengths, the dynamics of system \mathbf{y} is totally determined by the dynamics of system \mathbf{x} . That is, the solutions of, say \mathbf{x} can be mapped into solutions of \mathbf{y} .

$$\mathbf{y} = \boldsymbol{\psi}(\mathbf{x})$$

290 where $\boldsymbol{\psi}$ is a function from the phase space of the system \mathbf{x} to the phase space of system \mathbf{y} . When this
 291 happens we have generalized synchronization between these two systems. CS is a particular case of GS
 292 when $\boldsymbol{\psi}$ is the identity.

293 To detect a functional relation between two systems in generalized synchronization, Rulkov and co-
 294 workers proposed a technique called mutual false nearest neighbours [110]. The main idea is the see how
 295 nearby points are mapped under the dynamics. By studying the properties of nearby points one can infer
 296 the existence of the mapping $\boldsymbol{\psi}$. Here, we focus on another approach that turns the GS problem into a CS
 297 problem. This is the auxiliary system approach [1, 61]. The master system drives the slave system and an
 298 auxiliary system (copy of the slave). If the two copies of the slave exhibit CS then the master and slave are
 in GS.[1, 61]. An illustration of this scheme can be found in See Fig. 9.

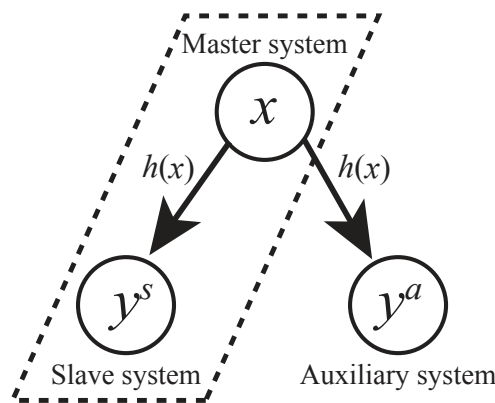


Figure 9.: Scheme of the auxiliary system approach for the generalized synchronization. Originally we only have the system in the dashed line box which is master-slave system as in Sec. 2.2.1. Then we add an auxiliary (helper) system \mathbf{y}^a . If there is CS between \mathbf{y}^s and \mathbf{y}^a , then the GS occurs between \mathbf{x} and $\mathbf{y}^{a,s}$.

299

Necessary conditions for the occurrence of GS for the system given by Eq. (31) is introduced by Kocarev and Parlitz as following: for all $(\mathbf{x}_0, \mathbf{y}_0) \in B$, where \mathbf{x}_0 and \mathbf{y}_0 are states for the master-slave systems at time $t = 0$ and B is the basin where all the trajectories approach to a manifold

$$M_\psi = \{(\mathbf{x}, \mathbf{y}) : \mathbf{y} = \psi(\mathbf{x})\}.$$

If M_ψ is attractive, different trajectories of the slave system will converge to the trajectory lying in M and it is determined only by \mathbf{x} . In other words, if the master drives a slave \mathbf{y}_0^s and an auxiliary (copy of slave) \mathbf{y}_0^a systems simultaneously, the driven ones must be completely synchronized $\forall \mathbf{y}_0^s, \mathbf{y}_0^a \in B_y$ we have

$$\lim_{t \rightarrow \infty} \|\mathbf{y}_t^s - \mathbf{y}_t^a\| = 0.$$

300 **Example:** Consider two identical Rössler systems (Eq. (17)) with the parameters ($a = 0.2, b = 0.2$ and
 301 $c = 5.7$) are driven by a Lorenz system (Eq. (14)) with the classical parameters ($\rho = 28, \sigma = 10$ and
 302 $\beta = 8/3$) via x -components. We used the auxiliary system approach the detect the critical coupling for GS.
 303 Indeed, numerical results showed that $\alpha_c \approx 0.12$ as seen in the synchronization diagram Fig. 10. For given
 304 $\alpha = 0.06$ CS is not observed between the slave systems therefore there is no GS between master and slave
 305 systems as well Fig. 11a. For a coupling constant larger than the critical one $\alpha = 0.2$ the slave and the
 306 auxiliary system display CS. Hence GS can be observed between master-slave system Fig. 11b.

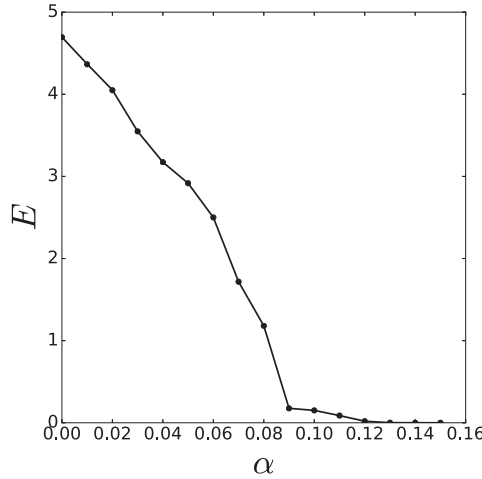


Figure 10.: Generalized Synchronization: Averaged over 300 realisations, time=4000 and time step=0.01

307 *2.4.1. Generalized Synchronization between diffusively coupled oscillators*

308 To gain some insight on this, we will use some ideas put forward by [51, 52]. This approach allows us to
 309 obtain a analytical understanding of the critical coupling associated with the transition to GS. Consider a
 310 master-slave system diffusively coupled.

$$\begin{aligned} \dot{\mathbf{x}} &= \mathbf{f}(\mathbf{x}) \\ \dot{\mathbf{y}} &= \mathbf{g}(\mathbf{y}) + \alpha \mathbf{H}(\mathbf{x} - \mathbf{y}) \end{aligned} \tag{31}$$

where \mathbf{H} is a positive definite matrix. We can write the slave equation as

$$\dot{\mathbf{y}} = \bar{\mathbf{g}}(\mathbf{y}) + \alpha \mathbf{H} \mathbf{x}$$

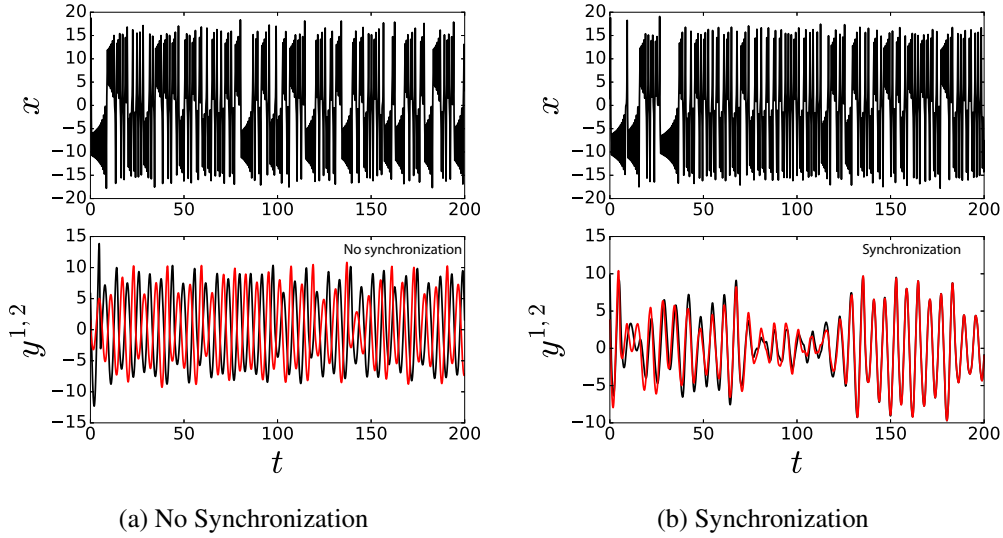


Figure 11.: Two simulations for the generalized coupling scheme: a Lorenz system \mathbf{x} drives two Rössler systems $\mathbf{y}^{s,a}$. The critical transition coupling is $\alpha_c \approx 0.12$. (a) For the coupling constant $\alpha = 0.06$, there is no synchronization since $\alpha < \alpha_c$ (b) for $\alpha = 0.2$ synchronization is obtained since $\alpha > \alpha_c$.

311 where $\bar{\mathbf{g}}(\mathbf{y}) = \mathbf{g}(\mathbf{y}) - \alpha \mathbf{H}\mathbf{y}$. The equation then splits into contributions solely coming from the slave and the
 312 driver. Now consider two copies of the slaves \mathbf{y}_1 and \mathbf{y}_2 . Because we know the system will exhibit GS when
 313 the copies of the slaves synchronize, we introduce a variable $\mathbf{z} = \mathbf{y}_1 - \mathbf{y}_2$. The system will undergo GS when
 314 $\mathbf{z} \rightarrow \mathbf{0}$. Differentiating we obtain

$$\dot{\mathbf{z}} = \mathbf{U}(t)\mathbf{z} - \alpha \mathbf{H}\mathbf{z}, \quad (32)$$

where we used the mean value theorem [55] to express

$$\mathbf{U}(t)\mathbf{z} = \mathbf{g}(\mathbf{y}_1(t)) - \mathbf{g}(\mathbf{y}_1(t) + \mathbf{z}(t)) = \left(\int_0^1 D\mathbf{G}(\mathbf{y}_1(t) + s\mathbf{y}_2(t)) ds \right) \mathbf{z}(t)$$

Notice that for the difference \mathbf{z} the driving term $\mathbf{H}\mathbf{x}$ disappears as it is common for both copies of the slave \mathbf{y}_1 and \mathbf{y}_2 . The only part of the coupling remaining is the term $-\alpha \mathbf{H}\mathbf{z}$, which adds an extra damping and provides dissipation. The trivial solution of \mathbf{z} is globally stable if the coupling is large enough. Indeed, we can construct a Lyapunov function for \mathbf{z} . Indeed, consider

$$V(\mathbf{z}) = \frac{1}{2} \langle \mathbf{z}, \mathbf{z} \rangle,$$

315 and differentiating the Lyapunov function along the solution $\mathbf{z}(t)$ of Eq. (32) we obtain

$$\frac{dV(\mathbf{z}(t))}{dt} = \langle \dot{\mathbf{z}}(t), \mathbf{z}(t) \rangle \quad (33)$$

$$\leq (\|\mathbf{D}\mathbf{g}\| - \alpha \lambda_{\min}(\mathbf{H})) \|\mathbf{y}\|^2 \quad (34)$$

where $\lambda_{\min}(\mathbf{H})$ is the minimum eigenvalue of \mathbf{H} . In this last passage, we used the Cauchy Schwartz inequality $|\langle \mathbf{U}(t)\mathbf{z}, \mathbf{z} \rangle| \leq \|\mathbf{U}(t)\mathbf{z}\| \|\mathbf{z}\| \leq \|\mathbf{U}\| \|\mathbf{z}\|^2$, and noticed that $\|\mathbf{U}\| \leq \|\mathbf{D}\mathbf{g}\|^1$. We also used the fact that \mathbf{H} is

¹We are using the uniform operator norm $\|\mathbf{U}\| = \sup_{t \geq 0} \|\mathbf{U}(t)\|$.

positive $\langle \mathbf{H}\mathbf{z}, \mathbf{z} \rangle \geq \lambda_{\min}(\mathbf{H})\|\mathbf{z}\|^2$. Hence, for

$$\alpha > \alpha_c = \frac{\|D\mathbf{g}\|}{\lambda_{\min}(\mathbf{H})}$$

the derivative of the Lyapunov function is negative and every solution of the system sinks to zero.

What did we learn? When $\alpha > \alpha_c$ we have GS. Any two trajectories of the slave \mathbf{y}_1 and \mathbf{y}_2 will converge towards the same asymptotic state. This happens because the coupling terms adds extra dissipation. The convergence rate is exponential $\|\mathbf{y}_1(t) - \mathbf{y}_2(t)\| \leq Ke^{-\eta t}$ because $\dot{V} \leq \eta V$ and η is uniform on the trajectories $\mathbf{y}_1, \mathbf{y}_2$ and \mathbf{x} . As a conclusion, there a function ψ such that the dynamics of the slave can be as $\mathbf{y} = \psi(\mathbf{x})$.

In the literature, a typical way to estimate whether one has GS is to compute the Lyapunov exponents of the slaves. Since we are assuming that the uncoupled systems are chaotic, for $\alpha = 0$ the slave will have a positive Lyapunov exponents. As we increase α the maximum Lyapunov exponent may become negative for a value α_c . We use this α_c as an estimate for the critical coupling for GS.

2.5. Summary of Synchronization types

We discuss the three cases commonly found in applications. A schematic representation of the cases is found in Fig. 15.

Complete synchronization in identical systems. If the isolated dynamics are identical, $\mathbf{f}_1 = \mathbf{f}_2$ and diffusively coupled, hence, the subspace $\mathbf{x}_1 = \mathbf{x}_2$ is invariant under Eq. (6). Indeed, the coupling vanishes and both systems will oscillate in unison for all coupling strengths α and all times. Such collective motion is called complete synchronization (CS). The question is whether CS is attractive, that is, if the oscillators state are nearly the same $\mathbf{x}_1(0) \approx \mathbf{x}_2(0)$, will they synchronize? Meaning that

$$\lim_{t \rightarrow \infty} \|\mathbf{x}_1(t) - \mathbf{x}_2(t)\| = 0.$$

See Fig. 12 for an illustration. In Sec 2.2, the CS was discussed in detail.

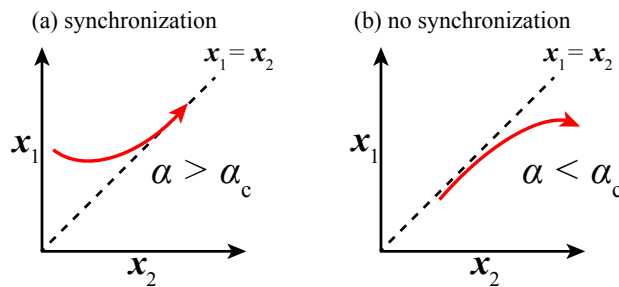


Figure 12.: Illustration of complete synchronization. (a) If the coupling strength is large enough ($\alpha > \alpha_c$), the systems converge to invariant synchronization manifold ($\mathbf{x}_1 = \mathbf{x}_2$), (b) otherwise ($\alpha < \alpha_c$), they diverge hence no synchronization.

Phase synchronization (PS) when $\mathbf{f}_1 \approx \mathbf{f}_2$. In this situation the subspace $\mathbf{x}_1 = \mathbf{x}_2$ is not invariant. And each system will have its own frequency given by their phase dynamics $\phi_{1,2}$. For small coupling strengths the phases can be locked $\phi_1 \approx \phi_2$ while the amplitudes remain uncorrelated Fig. 13. This phenomenon is called phase synchronization. Typically, the critical coupling for PS is proportional to the mismatch $\mathbf{f}_1 - \mathbf{f}_2$, as illustrated in Fig. 15. Further details were given in Sec. 2.3.

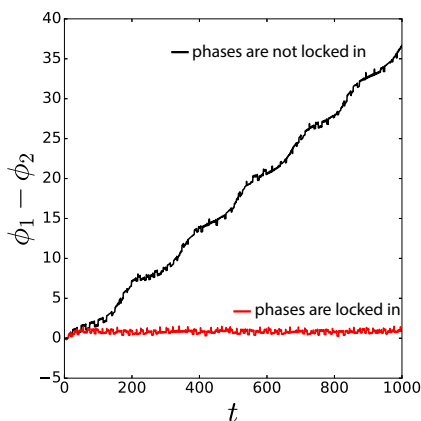


Figure 13.: Illustration of phase synchronization for two coupled slightly different and chaotic systems ($f_1 \neq f_2$). The evolution of the phase differences between the systems for two different coupling constants $\alpha < \alpha_c$ and $\alpha > \alpha_c$.

337 **Generalized synchronization** in master slave configurations. If the vector fields are different $f_1 = f$
 338 and $f_2 = g$, the systems can synchronize, but in a generalized sense. We consider systems coupled in a
 339 master-slave configuration. For certain coupling strengths, the dynamics of the master x can determine the
 340 dynamics of the slave y , that is $y = \psi(x)$, see Fig. 14. This is called *Generalized Synchronization* (GS).
 341 Further details for GS was given in Sec. 2.4.

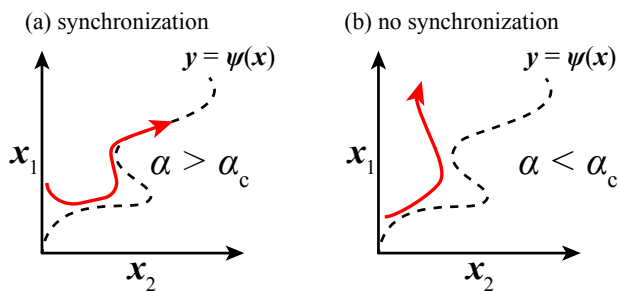


Figure 14.: Illustration of generalized synchronization. If the coupling strength is large enough, a functional relationship ($y = \psi(x)$) exhibits between the dynamical variables x_1 and x_2 . (a) If $\alpha > \alpha_c$, the generalized synchronization is observed (b) otherwise $\alpha < \alpha_c$, there is no generalized synchronization.

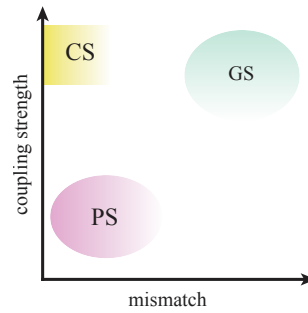


Figure 15.: Diagram of synchronization types for diffusively coupled systems. The horizontal axis depicts the mismatch between the isolated dynamics (f_1 and f_2) and the vertical axis the coupling constant. The diagram shows the typical balance between mismatch and coupling strength and to achieve a certain kind of synchronization. Complete synchronization (CS) occurs for identical chaotic systems ($f_1 = f_2$) and large enough coupling strengths. Phase synchronization (PS) is observed between slightly different systems for small coupling strengths. Generalized synchronization (GS) is a result of master-slave system and can occur for large mismatch parameters or even between distinct systems when the coupling strength large enough.

342 **2.6. Historical Notes**

343 Studies on synchronization dates back to Christiaan Huygens who studied coupled pendulums. In this case,
 344 the pendulums are periodic and have distinct frequencies, but due to interaction they adjust their rhythm.
 345 In the seventies, thanks to the works of Winfree [134] and Kuramoto [65] the area experienced a boom. In
 346 early 2000's many excellent books and reviews were devoted to this subject [5, 6, 9, 57, 101, 107, 123].

347 Chaotic synchronization on the other hand is younger. To begin with, the establishment and full accep-
 348 tance of the chaotic nature of dynamics is fairly new [40]. The role of chaos in nature was object of intense
 349 debate in the seventies when Ruelle and Takens proposed that turbulence was generated by chaos.

350 The chaotic dynamics can be fairly complicated. Typically, the evolution never repeats itself, nearby
 351 points drift apart exponentially fast, but in the long run the dynamics return arbitrarily close to its initial
 352 state. Such dynamics is so unpredictable that modern approach tackles it from a probabilistic perspective.

353 Given this complexity many researchers thought it is unlikely one could possibly synchronize two chaotic
 354 systems. How could a system with exponential divergence of nearby trajectories have a state were trajecto-
 355 ries come together while keeping their chaotic nature? That seemed paradoxal. Chaos and synchronization
 356 should not come together. This view was proven wrong in the late eighties. In fact, we have come to think
 357 it as rather natural. Funny enough, before this view was accepted synchronization of chaos had to be redis-
 358 covered a few times.

359 Back in the eighties, Fujisaka and Yamada had the first results on synchronization of chaos [38, 137, 138].
 360 They publish it in Japan, but their results went fairly unnoticed in the west. Just two years later mathe-
 361 maticians and physicists from Nizhny Novgorod exposed many of the concepts necessary for analyzing
 362 synchronous chaos [2]. This paper is now famous, but back then it also went largely unnoticed.

363 Only some years later the study of synchronization of chaos had its boom, largely as a result of the works
 364 by Pecora and Carroll [89]. Lou Pecora and co-workers went systematically tackling two coupled systems
 365 and then moved on to study chaotic systems coupled on periodic lattices [21, 47]. These early results were
 366 relying on ideas from Nuclear physics to diagonalize the lattice and stability theory (the Lyapunov methods)
 367 to analyze synchronization.

368 The nineties proved prolific for synchronization! Two groups proposed an extension of synchronization,
 369 the so-called generalized synchronization [1, 61–63, 110]. Generalized synchronization *only* asked for a
 370 functional relationship between the states, that is, the dynamics of one system is fully determined by the
 371 dynamics of the other. Also in the mid nineties, Rosenblum, Pikovsky and Kurths put forward the concept of

372 chaotic phase synchronization. Here two nearly identical chaotic oscillators can have their phase difference
 373 bounded while the amplitudes remain uncorrelated [108, 109].

374 A few years down the road, Pecora and Carroll were able to generalize their approach to undirected
 375 networks of diffusively coupled systems [91]. They also wrote a review about their approach [92]. These
 376 results open the door to the understanding of the role of the linking structure on the stability of synchrono-
 377 zation. Barahona and Pecora [14] showed that small-world networks are easier to globally synchronize
 378 than regular networks. Motter and coworkers [75, 76, 82, 141] showed that heterogeneity in the network
 379 structure may hinder global synchronization. On the other hand, Pereira showed such heterogeneity may
 380 enhanced synchronization of highly connected nodes [95].

381 3. Applications

382 In this section, we discuss the role of synchronization phenomena in various applications including secure
 383 communication approaches, parameter estimation of a model from data and prediction.

384 3.1. Secure Communication Based on Complete Synchronization

385 The first approach is to send an *analog* message [84]. The key idea is the following: the sender adds
 386 the message $m(t)$ on a chaotic signal $x(t)$ and generate a new signal $s(t) = m(t) + x(t)$ (Fig. 16). The
 387 assumption is that the amplitude of $x(t)$ is much larger than the amplitude of $m(t)$. This method is called the
 388 masking information on bearing signals. Because chaotic signals are noise-like and broadband (have many
 389 frequencies), it is difficult to read the message. One could then retrieve the message using synchronization.

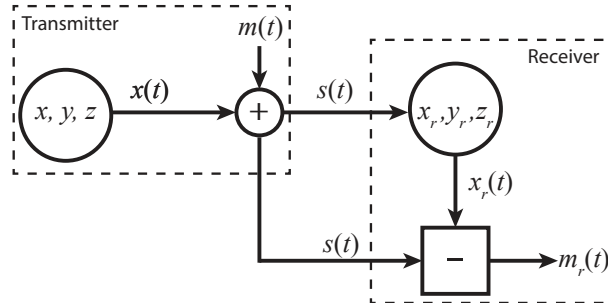


Figure 16.: Illustration of the message masking on bearing signal scheme. Transmitter generates a chaotic signal $x(t)$ and add the message $m(t)$ on it. This combined two signals $s(t) = x(t) + m(t)$ is sent to the receiver and both systems synchronize. Discarding the synced signal x_r from the s , the message $m_r \sim m$ is restored.

390 Masking of messages on bearing signals does not require encryption. Here is the keystone is selection
 391 of the transmitter and receiver systems such that they synchronize. They are also assumed to be identical
 392 (this means that the receiver knows the parameters of the transmitter). One can retrieve the message if the
 393 parameters are known. So, the parameters play a role of encryption key.

394 We illustrate this communication scheme using the Lorenz system Eq. (14). The Lorenz system has the
 395 particularity that it divided into subsystems (x, z) and (y, z) . We can use the variables x or y of a subsystem
 396 to drive the other subsystem. In this driving setting the synchronization between driver and slave is expo-
 397 nentially stable provided that the parameters σ , ρ and β are identical. Here, we have chosen x component
 398

399 to act as a driver. The message $s(t)$ drives the receiver system as

$$\begin{aligned} \dot{x}_r &= \sigma(y_r - x_r) \\ \dot{y}_r &= s(\rho - z_r) - y_r \\ \dot{z}_r &= -\beta z_r + sy_r. \end{aligned} \tag{35}$$

400 Since the synchronization of chaotic systems is exponentially stable for such system [89, 90] under low
 401 amplitude of noise the synchronization (coherence) still occurs. Then the chaotic signal x_r can be obtained
 402 from Eq. 35. Therefore the message can be regenerated by $m(t) = s(t) - x_r(t)$ (Fig. 16).
 as a message we use the signal

$$m(t) = 0.1 \frac{\sin(1.2\pi \sin^2(t))}{\pi \sin^2(t)} \cos(10\pi \cos(0.9t)) + \xi$$

403 where ξ is a white noise Fig. 17(a). We attach this message on x -component of the Lorenz system Eq. (14)
 404 with parameters $\sigma = 16.0$, $\rho = 45.2$ and $\beta = 4.0$ then the information is masked on bearing signal s
 405 Fig. 17(b). By synchronization we restore the message $m_r \sim m$ (Fig. 17(c)). This secure communication ap-
 406 plication is also experimentally demonstrated by using Chua's circuits [59, 87] and Lorenz-like circuit [27].

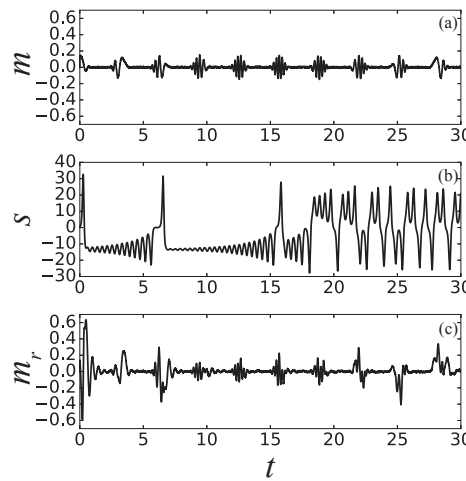


Figure 17.: The masking an analog message on bearing chaotic signal. (a) the low-amplitude message, (b) the message embedded into high-amplitude chaotic signal and (c) restored message from the transmitted signal.

407 The second approach is the modulation of the parameters for the *digital* communication. In this case,
 408 the message $m(t)$ only carries binary-valued signals. The setup is similar to the masking approach but
 409 the message is included in the transmitter parameters. The transmitter system has an adjustable parameter
 410 $\sigma_a(t) = \sigma + \delta m(t)$ such that we can tune the system into synchronization when $m(t) = 0$ and out synchro-
 411 nization when $m(t) = 1$ Fig. 18. We retrieve the message $m(t)$ by the synchronization and desynchronization
 412 pattern.

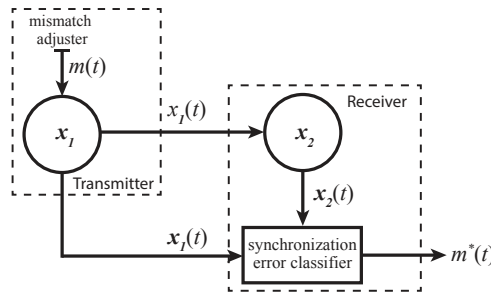


Figure 18.: A secure communication scheme: hiding a digital message on a chaotic signal. Changing a parameter of transmitter causes different level of synchronization errors between the transmitter and the receiver. The amplitude of the error E brings the message out.

413 The dynamics of transmitter and the receiver is given by

$$\begin{aligned}
 \dot{x}_1 &= \sigma_a(y_1 - x_1) \\
 \dot{y}_1 &= x_1(\rho - z_1) - y_1 \\
 \dot{z}_1 &= -\beta z_1 + x_1 y_1 \\
 \dot{x}_2 &= \sigma(y_2 - x_2) \\
 \dot{y}_2 &= x_1(\rho - z_2) - y_2 \\
 \dot{z}_2 &= -\beta z_2 + x_1 y_2
 \end{aligned}$$

414 where $\sigma_a = \sigma + \delta m(t)$ is the adjustable parameter. Again the key aspect is having mismatch between
 415 the transmitter and the receiver does not allow systems to synchronize. Modulating the parameter σ_a by
 416 the message $m(t)$ we can produce different levels of synchronization errors. Choosing the parameters of
 417 the transmitter and the receiver identical gives the synchronization error $E \sim 0$ (CS), this can be assigned
 418 binary 0 by $m(t) = 0$. The large mismatch δ causes a certain amount of synchronization error $E > 0$, this
 419 can be assigned binary signal 1 by $m(t) = 1$. Then the digital communication can be set between sender
 420 and receiver [26, 27].

421 Using same parameters as in the previous application ($\sigma = 16.0$, $\rho = 45.2$ and $\beta = 4.0$), we illustrate
 422 this digital communication. For this example, a digit of the message is set for 10 time units and the message
 423 is 0101010101 (Fig. 19(a)). For each message time, we change σ_a from σ to $\sigma + \delta$ and other way round.
 424 Then the synchronization error E varies according to this change (Fig. 19(b)). Due to change in the E , the
 425 message is restored (Fig. 19(c)).

426 There are more communication applications using the synchronization mechanism e.g. using hyper-
 427 chaotic systems [21, 29, 62, 94] or volume-preserving maps [22]. The common idea of all these given
 428 approaches is the CS phenomena, negative conditional Lyapunov exponent between the systems are needed
 429 to exhibit of the synchronization [89, 90].

430 3.2. Secure Communication Based on Phase Synchronization

431 Security is an important issue for communication approaches. As might be expected, some methods were
 432 improved and reported to break the CS based communication schemes [30, 88, 100, 115]. Then more secure
 433 communication scheme demonstrated by means the PS [23].

434 The scheme based on the PS possesses three chaotic Rössler systems $(x_{1,2,3})$. The transmitter of the
 435 scheme consists of two weakly coupled identical systems x_1 and x_2 over their x -components Eq. (36) and
 436 the receiver x_3 has slightly different dynamics. In this case, we couple the systems with using their phases
 437 Eq. (36) as presented in Ref. [24]. The phase definition for Rössler system is given by Eq. (22). The mean
 438 of two systems' phases ϕ_1 and ϕ_2 in transmitter can be used as a spontaneous phase signal ϕ_m to couple the

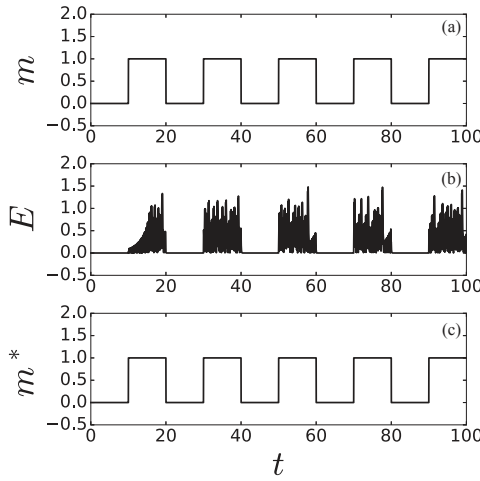


Figure 19.: Manipulating the parameter of a transmitter allows digital secure communication. In this application 10 time units are used for a single digit. (a) Digital message (0101010101), (b) the synchronization error and (c) restored message.

439 third system as in Eq. (36). As distinct from the CS based schemes, we have three systems and the reason
 440 behind these to improve the security. The return maps of the phase ϕ_m is way more complex than ϕ_1 (or ϕ_2),
 441 this makes to break dynamics not trivial [23].

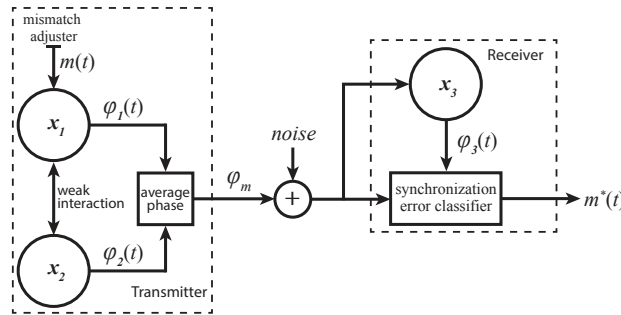


Figure 20.: A secure communication scheme by phase synchronization: hiding a digital message on a chaotic signal.

442 We illustrate this application by

$$\begin{aligned}
 \dot{x}_{1,2} &= -(\omega + \Delta\omega)y_{1,2} - z_{1,2} + \varepsilon(x_{2,1} - x_{1,2}) \\
 \dot{y}_{1,2} &= x_{1,2} + ay_{1,2} \\
 \dot{z}_{1,2} &= b + z_{1,2}(x_{1,2} - c) \\
 \dot{x}_3 &= -y_3 - z_3 + \alpha(r_3 \cos \phi_m - x_3) \\
 \dot{y}_3 &= x_3 + ay_3 \\
 \dot{z}_3 &= b + z_3(x_3 - c)
 \end{aligned}
 \tag{36}$$

where constant $\omega = 1$ and standard parameters of the Rössler system $a = 0.15$, $b = 0.2$ and $c = 10.0$. Coupling constants $\varepsilon = 5 \times 10^{-3}$ is between x_1 and x_2 , and α is between the transmitter and the receiver. r_3 is the amplitude of the response system given by Eq. (23). $\Delta\omega$ is the adjustable mismatch parameter, for

this illustration we select

$$\Delta\omega = \begin{cases} 0.01 & \text{if bit digit} = 1 \\ -0.01 & \text{if bit digit} = 0. \end{cases}$$

443 Similar to digital communication by the CS (see Section 3.1), the modulation of parameters in the trans-
 444 mitter would hide a binary message $m(t)$ on ϕ_m . The PS will exhibit between ϕ_m and ϕ_3 . Due to the changes
 445 on the adjustable control parameters $\Delta\omega$, the phase difference between ϕ_m and ϕ_3 varies. In other words,
 446 the phases are locked on different phase shifts. The message can be retrieved from different phase locking
 447 values (Fig. 20).

448 Because of the weak coupling, the CS never occurs Fig. 21(a). Every 10 time unit we switch $\Delta\omega$ param-
 449 eter to create a digital message $m(t)$ (010101...) Fig. 21(b). The hidden message on chaotic signal can be
 450 restored from the receiver using the phase difference between ϕ_m and ϕ_3 . If the message digit is 0, then the
 451 phase difference oscillates most time below 0, otherwise above 0 Fig. 21(c). Therefore it is easy to restore
 associated message m^* Fig. 21(d).

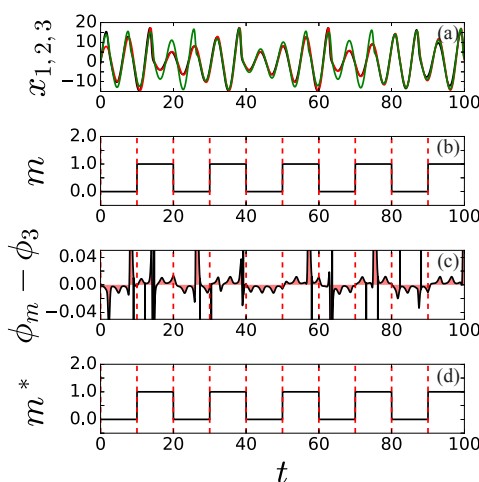


Figure 21.: An illustration for the secure communication by phase synchronization: hiding a digital message on a chaotic signal.

452 In real world examples, it is almost not possible to create identical systems, and the noise is always an
 453 issue to deal. The phase locking can be still preservable under effect of a certain level of noise.
 454

455 3.3. Parameter Estimation and Prediction

456 Now we have data and we want to learn about the system that generated the data. Thus we will be able to
 457 predict the future behaviours and critical transitions. The determining equations of the system are known
 458 however the parameters are not. The goal is to find these unknown parameters with using synchronization
 459 phenomena. So, we blend the data with equations. The data is then used to drive the equations. If they and
 460 coupled in a proper way (Sec. 2.2.1), the equations can synchronize with data. The key point is the fol-
 461 lowing: if the parameters of slave system are identical with the master whose produced driving signal, then
 462 the CS exhibits (synchronization error $E = 0$) otherwise no CS (synchronization error $E > 0$). Therefore,
 463 it is possible to estimate the parameters by a strategy to minimize the synchronization error $E \rightarrow 0$ such as
 464 POWELL technique [103].

465 We assumed that we have a limited data and we want to predict the future of the system. After the
 466 parameters are estimated, the state of the synchronized slave matches the data. Because the solution of the
 467 equations are then the same as the data, we can use the equations to predict future dynamics.

468 The second approach is to estimate a slave system's parameters of a master-slave system. In this case,
 469 the dynamics of master and slave is distinct. We assume that we have two given datasets: one of them from
 470 master system and the other one is from the slave. The governing dynamics of the master-slave system is
 471 given

$$\begin{aligned}\dot{x} &= f(x) \\ \dot{y} &= g(y) + h(x,y)\end{aligned}$$

472 where x and y are the states of master and slave systems respectively. We aim to estimate the parameters of
 473 g . Here we cannot use y data to drive another g system directly as in previous approach since y is driven by
 474 x . If we know that master-slave system is in the GS and the coupling function h is known, then we can apply
 475 the auxiliary system approach which is the master system drives an auxiliary (copy of the slave) z Fig. 22.
 476 We expect that the CS exhibits between the slave y and auxiliary z systems if the parameters are identical.
 Using the GS idea, the problem turned into the CS problem. From now on, minimizing the synchronization

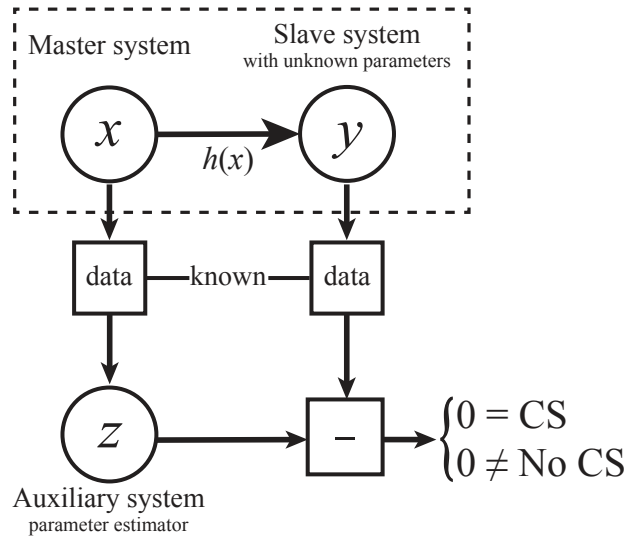


Figure 22.: Only two data sets are known from a master-slave system, into the dashed rectangle, without any info about the parameters. An auxiliary system is driven by the data from the master and measure the amplitude difference between the auxiliary and the data from the slave system. If the difference is 0, then there is a CS that means the parameters of the slave and the auxiliary are identical.

477 error $E \rightarrow 0$ technique can be used to estimate the unknown parameters. Similar to the previous approach,
 478 the future of the system can be predicted as well.

480 **Example:** Consider a Lorenz system with classical parameters is driven by a Rössler system. We have
 481 only two data sets, x_1 -component of the Rössler (Eq. (17)) and y_1 -component of the Lorenz (Eq. (14)).
 482 Then we drive an auxiliary system z by x_1 as

$$\begin{aligned}\dot{z}_1 &= \sigma_e(z_2 - z_1) + \alpha(x_1 - z_1) \\ \dot{z}_2 &= z_1(\rho_e - z_3) - z_2 \\ \dot{z}_3 &= -\beta_e z_3 + z_1 z_2.\end{aligned}$$

483 The goal is to find the parameters of slave system. The spontaneous synchronization error is

$$E(t) = \|z_1 - y_1\|. \tag{37}$$

484 Adjusting the parameters of $z(\sigma_e, \rho_e, \beta_e)$ we minimize the simultaneous error $E(t)$ by Powell's algorithm [103]. This method allows us to estimate the parameters of the slave system (Fig. 23).

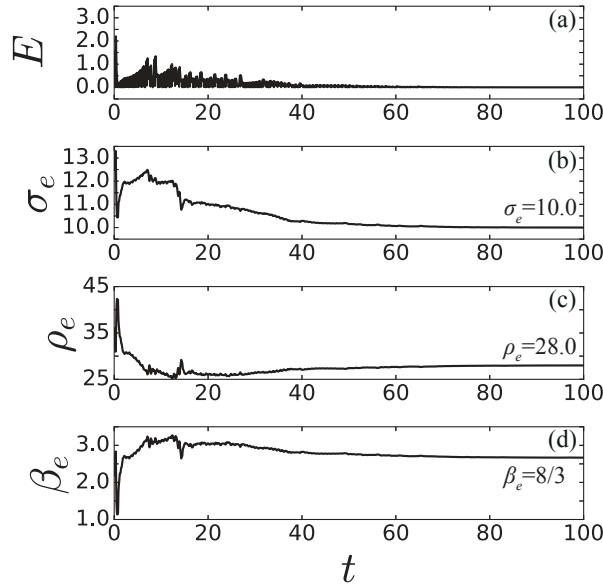


Figure 23.: Illustration of parameter estimation. Standard parameters of Lorenz system.

485

486 3.4. Chaos Anticipation

487 Chaos is unpredictable but synchronization can help predicting the state of a chaotic system ahead of time.
 488 Anticipating synchronization (AS) is a good approach for the future prediction since the slave system
 489 synchronizes with the upcoming states of the master system at time $t + \tau$ where τ is a time delay. The
 490 occurrence of AS depends on the coupling constant α . Therefore it is not dependent on isolated dynamics
 491 or time delay τ and regarding to type of desired application higher dimensional chaotic systems can be
 492 used for an arbitrary time delay. This anticipation of chaos can be used or is used in applications such as
 493 semiconductor lasers with optical feedback, secure communications [70].

Consider two chaotic systems in a master-slave interaction and the master has a certain delay τ feedback Fig. 24. Because of the internal delay feedbacks, it may well happen that the master x and slave y synchronize but with some time delay

$$\mathbf{x}(t) = \mathbf{y}(t - \tau)$$

When this happens we have

$$\mathbf{y}(t) = \mathbf{x}(t + \tau).$$

494 Hence, although the system x is fully chaotic, we can precisely predict its future state from the system
 495 y . In other words the slave system anticipates the master system. This kind of synchronization is called
 496 anticipated synchronization (AS).

497 **Example:** We consider two coupled Ikeda equations,

$$\begin{aligned} \dot{x} &= -\alpha x - \mu \sin x_\tau \\ \dot{y} &= -\alpha y - \mu \sin x \end{aligned} \tag{38}$$

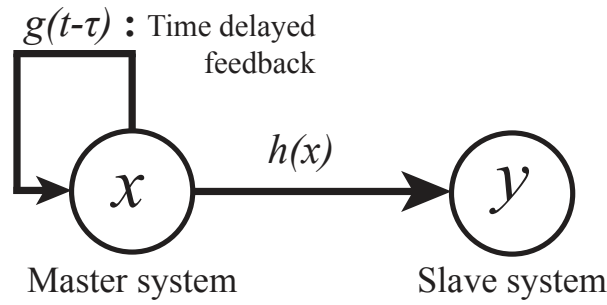


Figure 24.: Scheme of anticipating synchronization with memory in the driver systems

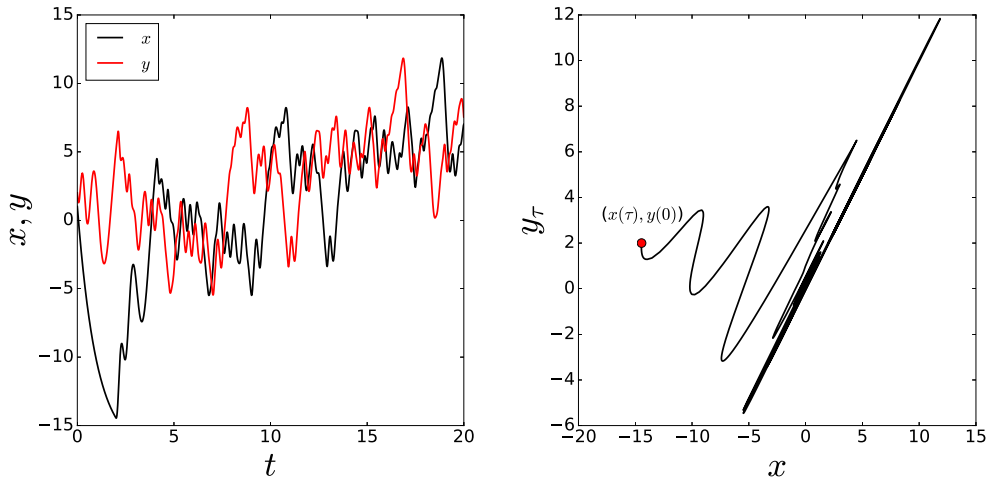
498 We use the notation $y_\tau = y(t - \tau)$. The scheme of the system is given in Fig. 24. The synchronization error
 499 for delayed system is given by,

$$z = x - y_\tau$$

500 and to show that synchronization is attractive we analyze the first variational equation

$$\begin{aligned} \dot{z} &= \dot{x} - \dot{y}_\tau \\ &= -\alpha x - \mu \sin x_\tau - (-\alpha y_\tau - \mu \sin x_\tau) \\ &= -\alpha z. \end{aligned} \tag{39}$$

501 The solution is $z(t) = z_0 e^{-\alpha t}$ and for $\alpha > 0$ the synchronization is globally exponentially stable.



(a) Time series of coupled Ikeda equations. (b) Phase space and synchronization manifold for x and y_τ .

Figure 25.: Anticipating chaotic synchronization. In the beginning, the systems are not in harmony. After a transient time both systems are getting into a time-delay τ synchronization. For this illustration $\tau = 2$. (a) time series of the systems (b) phase space and synchronization manifold of the system. The red circle is the initial condition for the trajectory of (x, y_τ) .

502 To illustrate AS, we simulate Eq. (38) with a fourth order Runge-Kutta integrator for the delay-differential
 503 equations for the parameters $\alpha = 1$, $\mu = 20$ and $\tau = 2$. The simulation starts from a random initial condition.
 504 After enough transient time t , the master x and the slave y systems synchronize with a time delay (τ)

505 Fig. 25(a). The transient time can be observed from the phase space of x and y_τ . The initial condition is
 506 given by a red circle in Fig. 25(b), the trajectory converges to the synchronization manifold ($x = y_\tau$).

507 **Example:** The AS can occur for higher dimensional chaotic system. For such cases the critical coupling
 508 constant can be positive ($\alpha_c > 0$). The AS can be obtained without delayed state in the master system, that
 is, without memory in the master system. The scheme of this model is given in Fig. 26. We can demonstrate

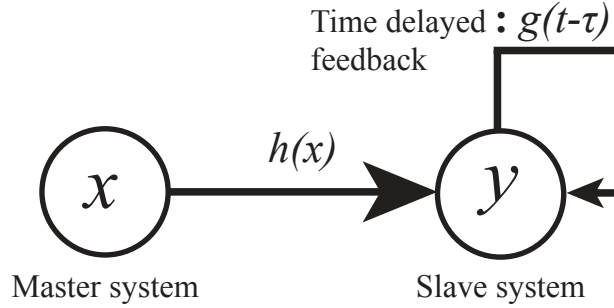


Figure 26.: Scheme of anticipating synchronization without memory in the driver systems

509 this case with Rössler system, the governing equations are given by
 510

$$\begin{aligned}
 \dot{x}_1 &= -x_2 - x_3 \\
 \dot{x}_2 &= x_1 + ax_2 \\
 \dot{x}_3 &= b + x_3(x_1 - c) \\
 \dot{y}_1 &= -y_2 - y_3 + \alpha(x_1 - y_{1,\tau}) \\
 \dot{y}_2 &= y_1 + ay_2 \\
 \dot{y}_3 &= b + y_3(y_1 - c)
 \end{aligned} \tag{40}$$

511 where the parameters are $a = 0.15$, $b = 0.2$ and $c = 10$. We simulate Eq. (40) for no AS ($\alpha < \alpha_c$) Fig. 27
 512 and AS ($\alpha > \alpha_c$) Fig. 27 cases. In this memoryless AS approach, the synchronization is also dependent on
 513 time delay τ .

514 4. Synchronization in complex networks

515 Synchronization is commonly found in networks of natural and mankind-made systems such as neural
 516 dynamics [16, 42, 116], cardiovascular systems [67, 114, 122], power grids [74], superconducting Joseph
 517 junctions [132]. The theory we presented in the previous chapters can be generalized to understand certain
 518 aspects of synchronization in these complex systems.

519 We will focus on diffusively interacting identical oscillators, so the dynamics of the coupled system reads
 520 as

$$\frac{d\mathbf{x}_i}{dt} = \mathbf{f}(\mathbf{x}_i) + \alpha \sum_{j=1}^N A_{ij} [\mathbf{H}(\mathbf{x}_j) - \mathbf{H}(\mathbf{x}_i)], \tag{41}$$

521 where $\mathbf{f}: \mathbb{R}^n \rightarrow \mathbb{R}^n$ describes the dynamics of the isolated system, α is the overall coupling strength, N is
 522 the number of oscillators, $\mathbf{H}: \mathbb{R}^n \rightarrow \mathbb{R}^n$ is the coupling function. Finally, A_{ij} dictates who is interacting with
 523 whom. $A_{ij} = 1$ if i receives a connection from j and 0 otherwise. The matrix \mathbf{A} (the dimension is $N \times N$)
 524 provides the network linking structure and it is called adjacency matrix. This matrix will play an clear role
 525 in the analysis.

526 The network dynamics of diffusively coupled system in Eq. (4) models many physical systems. A few
 527 specific examples are:

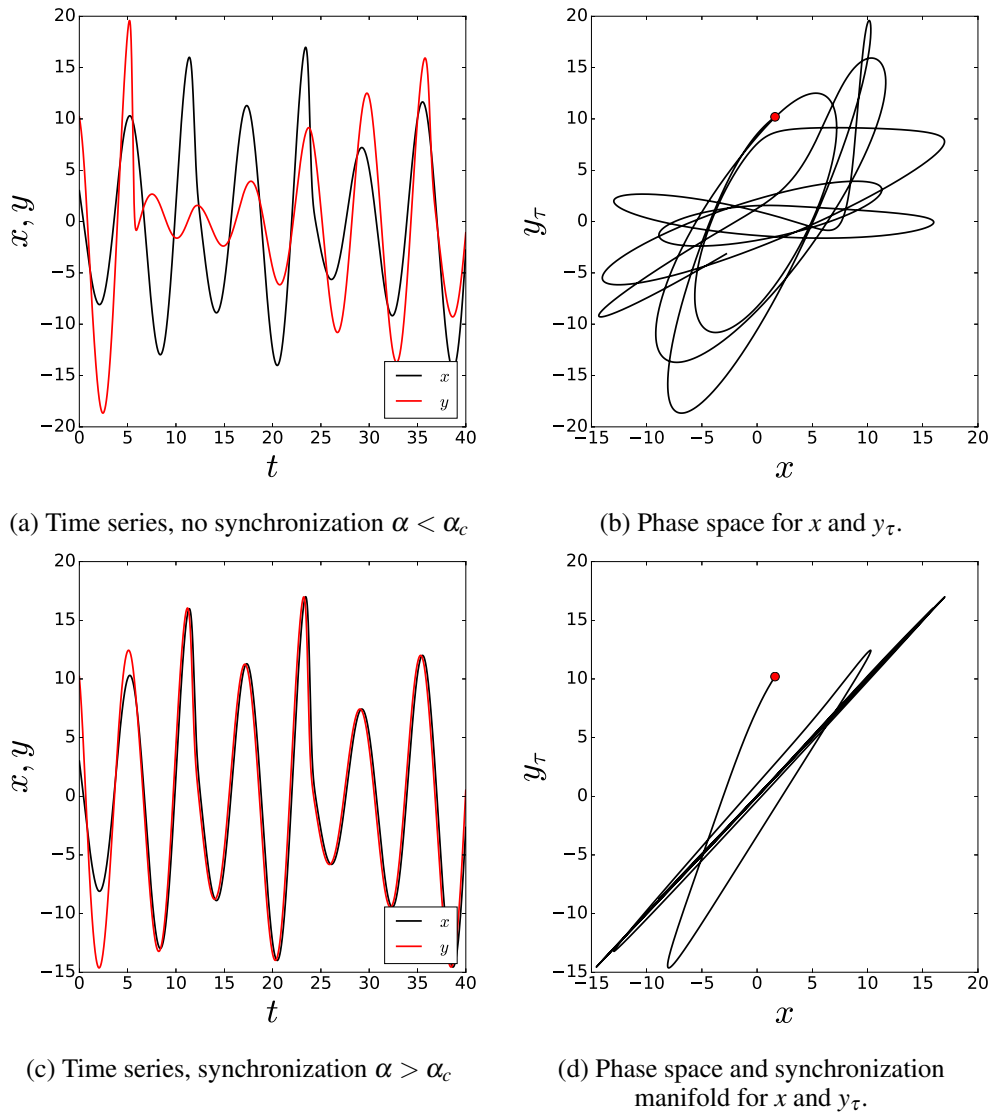


Figure 27.: Anticipating synchronization does not obtain for $(\alpha < \alpha_c)$, otherwise $(\alpha > \alpha_c)$ the AS exhibits. For this illustration the delay is selected as $\tau = 0.2$. (a) time series of the systems where $\alpha < \alpha_c$ and (b) phase space. (c) time series of the systems where $\alpha > \alpha_c$ and (d) phase space and synchronization manifold of the system. The red circle is the initial condition for the trajectory of (x, y_τ) .

528 **Electronic Circuits with Resistive interaction.** Electric circuits, e.g., Chua, Roessler-like, Lorenz-like,
 529 can be coupled over their resistors then Eq. models this system [89]. Another case, only one electric
 530 circuit can be driven by an external signal as master-slave system (for details, see Sec. 2.2.1)[12].

531 **Neuron Networks with Electrical Coupling.** In brain network, f can be the isolated neuron dynamics
 532 modelled by differential equations with chaotic or periodic behaviour and having different time-
 533 scales, that is, the isolated can have burst and single regime [50] and H the electrical synapses $H(\mathbf{x}_1 -$
 534 $\mathbf{x}_2) = (x_1 - x_2, 0, 0)$.

535 **Stable Biological System.** In biological systems when the isolated dynamics has a stable periodic motion
 536 then typically one can rephrase the network dynamics in terms of our model. For instance, the heart
 537 consists of millions of pacemaker cells. Each cell when isolated has its own rhythm, but when put
 538 together these cells interact and behave in unison to deliver the strong electrical pulse that make our
 539 heart beat [123]. The dynamics of the pacemaker cells are modelled by phase oscillators ϕ_i with

540 distinct frequencies ω_i and the coupling function is a simple sine function $H(\phi_1 - \phi_2) = \sin(\phi_1 -$
 541 $\phi_2)$ [112, 114].

542 **Laser Arrays.** Lasers can be arranged arrays or complex networks. In this case, one is interested in the
 543 electrical field dynamics. Such electrical field is govern by equations with interaction akin to diffusion
 544 Ref. [77]. So, the approach presented here can be extrapolated to such lasers under slight changes.

545 In fact, when we considering periodic oscillators ² the above model is a normal form for the networked
 546 system. That is, the isolated system has a periodic exponentially attracting orbit, we couple the system, and
 547 in the weak coupling regime, the amplitudes will change only slightly but the phases can change by large
 548 amounts. So the dynamics can be described only in terms of the phases. The phase description will again
 549 fit in our Eq. (4).

550 Our synchronization results given in the previous sections are exponentially stable. In other words, if once
 551 the trajectories are into the synchronization subset, the solution is robust and persistent to the perturbations.
 552 For N coupled nonidentical systems ($f_1 \neq f_2 \neq \dots \neq f_N$), complete synchronization is not possible. However,
 553 because of exponentially stable solutions, highly coherent state around the synchronization subset can be
 554 still observed [99, 127].

555 4.1. Interactions in terms of Laplacian

556 Because of the diffusive nature of the interaction, it is possible to represent the coupling in terms of the
 557 Laplacian matrix L . Indeed,

$$\begin{aligned} \sum_{j=1}^N A_{ij} [\mathbf{H}(\mathbf{x}_j) - \mathbf{H}(\mathbf{x}_i)] &= \sum_{j=1}^N A_{ij} \mathbf{H}(\mathbf{x}_j) - \mathbf{H}(\mathbf{x}_i) \sum_{j=1}^N A_{ij} \\ &= \sum_{j=1}^N A_{ij} \mathbf{H}(\mathbf{x}_j) - k_i \mathbf{H}(\mathbf{x}_i) \\ &= \sum_{j=1}^N (A_{ij} - \delta_{ij} k_i) \mathbf{H}(\mathbf{x}_j) \end{aligned}$$

558 where $k_i = \sum_{j=1}^N A_{ij}$ is the degree of the i th node, δ_{ij} is the Kronecker delta, and recalling that $L_{ij} =$
 559 $\delta_{ij} k_i - A_{ij}$ we obtain

$$\frac{d\mathbf{x}_i}{dt} = \mathbf{f}(\mathbf{x}_i) - \alpha \sum_{j=1}^N L_{ij} \mathbf{H}(\mathbf{x}_j). \quad (42)$$

560 Our results will depend on this representation and on the spectral properties of L .

Notice that

$$\mathbf{x}_1(t) = \mathbf{x}_2(t) = \dots = \mathbf{x}_N(t) = \mathbf{s}(t),$$

is an invariant state for all coupling strength α , because the laplacian is zero row sum. When $\alpha = 0$ the
 oscillators are decoupled, and Eq. (52) describes N copies of the same oscillator with distinct initial condi-
 tions. Since, the chaotic behavior leads to a divergence of nearby trajectories, without coupling, any small
 perturbation on the globally synchronized motion will grow exponentially fast, and lead to distinct behavior
 between the node dynamics. We wish to address the local stability of the globally synchronized state. That

²Or Rössler type oscillator where the phases are well defined and the coupling between chaotic amplitudes and phases are small

is, if all trajectories start close together would become synchronized

$$\lim_{t \rightarrow \infty} \|\mathbf{x}_i(t) - \mathbf{x}_j(t)\| = 0$$

561 The goal of the remaining exposition is to answer this question. Before, we continue with the analysis, we
 562 will briefly review some examples and constructions of graphs and discuss the relevant aspects necessary
 563 to tackle for problem.

564 **4.2. Relation to other types of Synchronization**

565 We will focus on the transition to complete synchronization, which is mainly related to Sec. 2.2. This is no
 566 severe restriction as in certain scenarios other types of synchronization can often be formulated in terms of
 567 our model.

568
 569 *Extension to Phase Synchronization.* As we discussed in the introduction of Sec. 4, if the dynamics of f is
 570 periodic then we can introduce a phase variable which will follow our main system of equations Eq. (4)
 571 as the phase reduction tells us that generically the interaction between phases are diffusive. Moreover,
 572 because our results will yield robust transition to synchronization, if the oscillators are nearly identical the
 573 phase synchronization will persist.

574
 575 *Extension to Generalized Synchronization.* Roughly speaking a form of generalized synchronization in net-
 576 works is the so-called pinning control, where one tries to control the behaviour of synchronized trajectories
 577 by driving the network with external nodes. One extends the network to include the driver node. Therefore,
 578 the theory necessary to tackle this problem is the same as presented here. The main question is how to
 579 connect the driver nodes in such a way that control is effective.

580 **4.3. Complex Networks**

581 A *network*, also called graph G in mathematical literature, is a set of N elements, called *nodes* (or vertices),
 582 connected by a set of M *links* (or edges) Fig. 28. Networks represent interacting elements and are all around
 583 from biological systems, e.g. swarm of fireflies, food webs or brain networks, to mankind made systems,
 e.g. the world wide web, power grids, transportation networks or social networks.

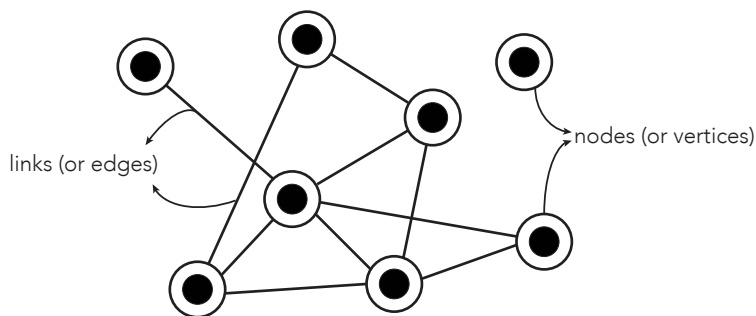


Figure 28.: A network visualisation with eight nodes and ten links.

584
 585 A *network is called simple* if the nodes do not have self-loops (i.e., nodes have connections to themselves).
 586 An illustration of a simple network is found in Fig. 29(a). A nonsimple network, therefore, containing
 587 connections is depicted in Fig. 29(d). We need a bit of technology from graph theory to make sense
 588 of our networks. A few basic notions are as follows

589 *A network is undirected* if there is no distinction between the two nodes associated with each link
 590 Fig. 29(a).

591 *A path in a network* is a route (sequence of edges) between connected nodes without repeating i.e. a path
 592 can visit a node only once. The length of a path is the number of links in the path. See further
 593 details in Ref. [20, 80]. In Fig. 30 we illustrate the paths of two selected (red) nodes in a network.
 594 Between two red nodes there are five different paths and each path is given in subplots of Fig. 30.
 595 The length of paths are five for Fig. 30(a), four for Fig. 30(b), three for Fig. 30(c) and (d), and two
 596 for Fig. 30(e). Therefore the shortest path length, also called *geodesic path*, between these two red
 597 nodes is illustrated in Fig. 30(e).

598 *The network diameter d* is the longest length of the shortest path between all possible pairs of nodes. In
 599 order to compute the diameter of a graph, first we find the shortest path between each pair of nodes.
 600 The longest length of all these geodesic paths is the diameter of the graph. If there is an isolated
 601 node (a node without any connections) or disconnected network components, then the diameter of
 602 the network is infinite. A network of finite diameter is called **connected** (Fig. 29(a)), otherwise **dis-**
 603 **connected** (Fig. 29(b)).

604 *A network is directed* if the links transmit the information towards only associated direction Fig. 29(c). If
 605 the graph is directed then there are two connected nodes say, u and v , such that u reachable from v ,
 606 but v is not reachable from u . See Fig. 29(c) for an illustration.

607 *A network is weighted* if links have different importance from each other or the links may be carry different
 608 amount of information. Such graphs are called *weighted* networks Fig. 29(d). Moreover, a network
 609 may have self-loops, that is, a node can affect itself as well Fig. 29(d).

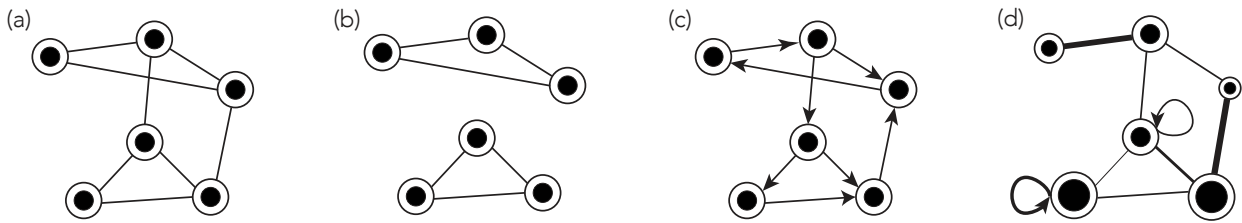


Figure 29.: Visualization of network types: (a) an unweighted simple network, (b) a disconnected network, (c) a directed network, (d) a weighted network with self-loops.

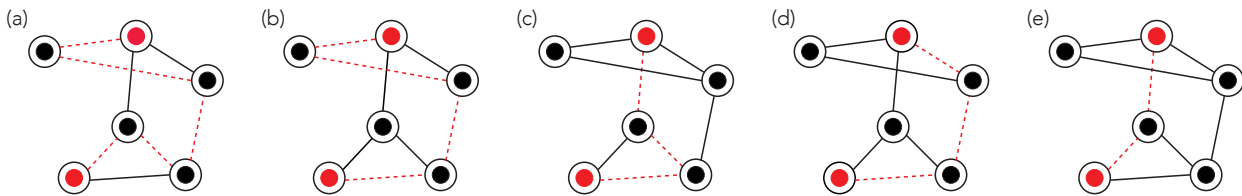


Figure 30.: Visualization of paths (red dashed) between two selected nodes (red) in a network: path length of (a) is five, (b) is four, (c) and (d) are three and (e) is two. Therefore the shortest path length for these two red nodes is two.

A graph can be described by its *adjacency matrix* A with $N \times N$ elements A_{ij} . The adjacency matrix A encodes the topological information, and is defined as $A_{ij} = 1$ if i and j are connected, otherwise 0. Therefore, the adjacency matrix of an undirected network is symmetric, $A_{ij} = A_{ji}$. The *degree* k_i of the i th node is the number of edges belongs to the node, defined as

$$k_i = \sum_j A_{ij}.$$

610 The *Laplacian matrix* L is another way to represent the network, defined as

$$L_{ij} = \begin{cases} k_i & \text{if } i = j \\ -1 & \text{if } i \text{ and } j \text{ are connected} \\ 0 & \text{otherwise.} \end{cases} \quad (43)$$

There is a direct relationship between the Laplacian L and the adjacency matrix A . In a compact form it reads

$$L_{ij} = \delta_{ij}k_i - A_{ij}$$

611 where δ_{ij} is the Kronecker delta, which is 1 if $i = j$ and 0 otherwise. We demonstrate some example network
 612 sketches with their adjacency A and Laplacian L matrices in Fig. 31.

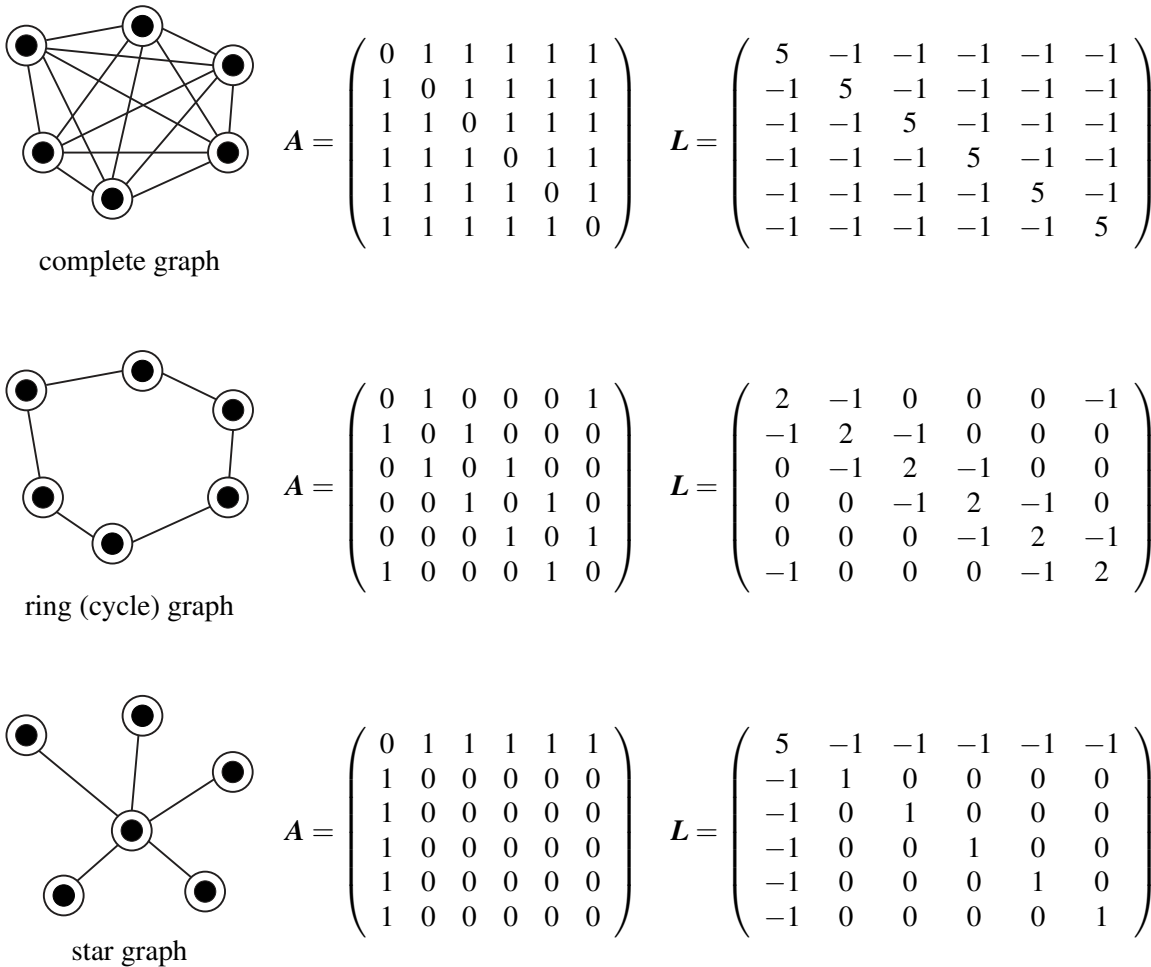


Figure 31.: Various network examples with six nodes. Their adjacency A and Laplacian L matrices.

613 The networks we encounter in real applications have a wilder connection structure. Typical examples are
 614 cortical networks, the Internet, power grids and metabolic networks [79, 80]. These networks don't have a
 615 regular structure of connections such as the ones presented in Fig. 31. We say that the network is *complex*
 616 if it does not possess a regular connectivity structure.

617 One of the goals is the understand the relation between the topological organization of the network and
 618 its relation functioning such as its collective motion.

619 **2k Regular Graph** is a standard graph model where each node has $2k$ links then the total number of links
 620 is $M = kN$ where N is total number of nodes Fig. 32 (a). This model is rather important one since
 621 the connections of spatiotemporal graphs, in general, connected to the nearest neighbours. $2k$ regular
 622 graph is an alternative representation of such models. It is important to mention that the graph model
 623 is fixed with given k and N therefore all properties of the graph is known analytically.
 624 **Erdős-Rényi** network is generated by setting an edge between each pair of nodes with equal probability
 625 p , independently of the other edges Fig. 33 (a). If $p \gg \ln N/N$, then a the network is almost surely
 626 connected, that is, as N tends to infinity, the probability that a graph on n vertices is connected tends
 627 to 1. The degree is pretty homogeneous, almost surely every node has the same expected degree [25].
 628 **Small World** network is a random graph model which possesses the small-world properties; i.e the average
 629 path length is short and clustering is large. The network is generated from a $2k$ regular graph, each
 630 link of the graph is rewired with a probability p . Therefore if $p = 0$ then the there is no rewiring and
 631 the graph is $2k$ regular. For $p = 1$ then each link is rewired i.e the graph is approaching to Erdős-
 632 Rényi network with $p = \frac{kN}{2\binom{N}{2}}$. The small-world properties come true between $0 < p < 1$ Fig. 32. In
 633 many real world networks, the properties of small-world topology can be obtained.

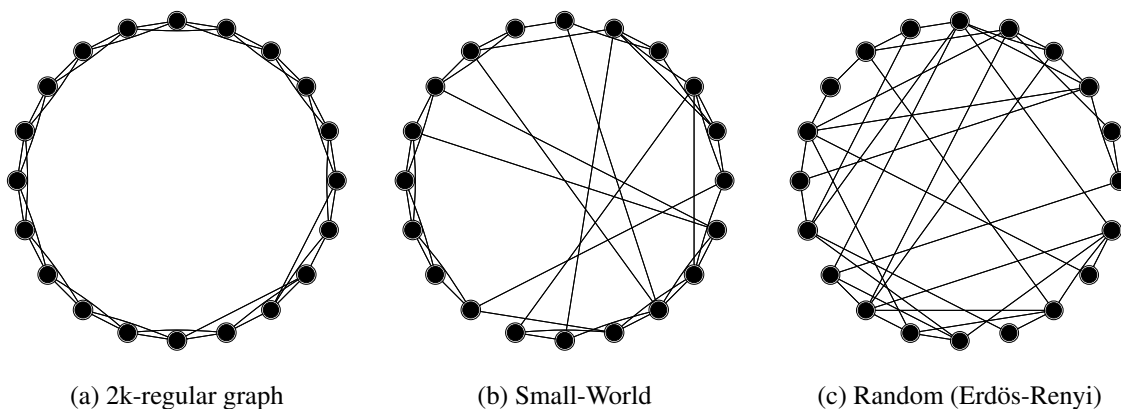


Figure 32.: Watts - Strogatz random network approach

634 **The Barabasi-Albert** network possesses a great deal of heterogeneity in the node's degree, while most
 635 nodes have only a few connections, some nodes, termed hubs, have many connections Fig. 33 (a).
 636 These networks do not arise by chance alone. The network is generated by means of the cumulative
 637 advantage principle – the rich gets richer. According to this process, a node with many links will have
 638 a higher probability to establish new connections than a regular node. The number of nodes of degree
 639 k is proportional to $k^{-\beta}$. These networks are called scale-free networks [79, 80]. Many graphs arising
 640 in various real world networks display similar structure as the Barabasi-Albert network [3, 4, 13].

641 **Hypercube graph** Q_m is a m -dimensional hypercube formed regular graph (Fig. 33 (b)). It is a regular
 642 graph since each node has m neighbours and total number of nodes is 2^m and edges is 2^{m-1} .

643 Random networks serve as a proxy to many applications as well as a surrogate. There are many nice
 644 ways to construct random network

645 **Configuration Model** is a random network model created by the degree distribution $P(k)$. If the degree
 646 distribution of a graph is known, then the nodes with associated number of links are known how-
 647 ever the connection structure between nodes is unknown. The nodes can be drawn with their stubs
 648 (half links) Fig. 34 (a), then randomly these stubs can be linked and two stubs create a proper link
 649 Fig. 34 (b). This process is a random matching, obviously different network structures can arise from
 650 this random process.

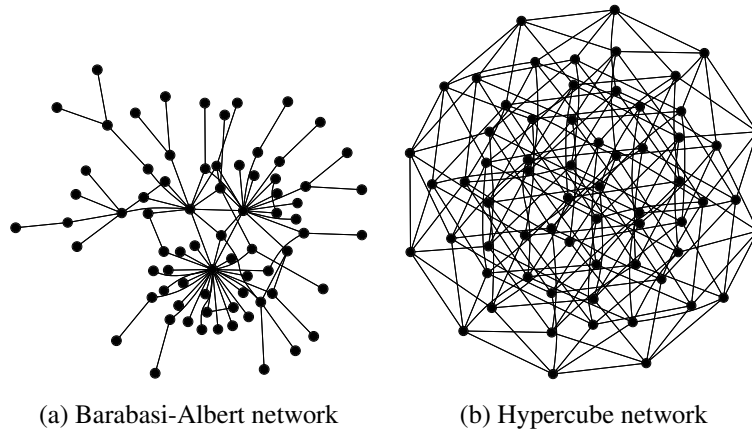


Figure 33.: Some examples of complex networks.

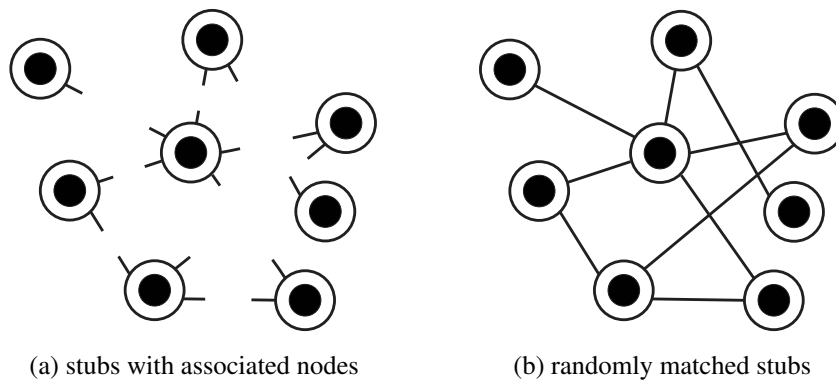


Figure 34.: Configuration model.

Expected degrees. Fix a network of N nodes and consider a vector

$$\mathbf{w} = (w_1, w_2, \dots, w_N),$$

In this model, each link A_{ij} between nodes i and j is an independent Bernoulli variable taking value 1 with success probability

$$p_{ij} = w_i w_j \rho,$$

and 0 with probability $1 - p_{ij}$, where

$$\rho = \frac{1}{\sum_{i=1}^N w_i}.$$

651

To ensure that $p_{ij} \leq 1$ it is assumed that $\mathbf{w} = \mathbf{w}(N)$ is chosen so that

$$\Delta^2 \rho \leq 1. \tag{44}$$

The *degree* $k_i = \sum_j A_{ij}$ of the i th is a random variable. An interesting property of this model is that

under this construction w_i is the expected value of k_i , that is,

$$\mathbb{E}_w(k_i) = \sum_j \mathbb{E}_w(A_{ij}) = w_i$$

652 So, the different to the configuration model is that we do not fix the node degree, but rather obtain the
653 degree probabilistically. This model also have many desirable concentration properties in the large N limit.

654 4.4. Spectral Properties of the Laplacian

655 The eigenvalues and eigenvectors of A and L tell us a lot about the network structure. The eigenvalues of L
656 for instance are related to how well connected is the graph and how fast a random walk on the graph could
657 spread. In particular, the smallest nonzero eigenvalue of L will determine the synchronization properties
658 of the network. Since the graph is undirected the matrix L is symmetric its eigenvalues are real, and L has
659 a complete set of orthonormal eigenvectors [41]. The next result characterizes important properties of the
660 Laplacian

661 **Theorem 1:** Let G be an undirected network and L its associated Laplacian. Then:

- 662 a) L has only real eigenvalues,
- 663 b) 0 is an eigenvalue and a corresponding eigenvector is $\mathbf{1} = (1, 1, \dots, 1)^*$, where $*$ stands for the trans-
664 pose.
- c) L is positive semidefinite, its eigenvalues enumerated in increasing order and repeated according to
their multiplicity satisfy

$$0 = \lambda_1 \leq \lambda_2 \leq \dots \leq \lambda_N$$

- 665 d) The multiplicity of 0 as an eigenvalue of L equals the number of connect components of G .

666 Therefore, λ_2 is bounded away from zero whenever the network is connected. The smallest non-zero
667 eigenvalue is known as algebraic connectivity, and it is often called the Fiedler value. The spectrum of the
668 Laplacian is also related to some other topological invariants. One of the most interesting connections is its
669 relation to the diameter, size and degrees.

670 **Theorem 2:** Let G be a simple network of size N and L its associated Laplacian. Then:

- 671 (1) [71] $\lambda_2 \geq \frac{4}{Nd}$
- 672
- 673 (2) [36] $\lambda_2 \leq \frac{N}{N-1}k_1$

674 We will not present the proof of the Theorem here, however, they can be found in references we provide
675 in the theorem. We suggest the reader to see further bounds on the spectrum of the Laplacian in Ref. [72].
676 Also Ref. [73] presents many applications of the Laplacian eigenvalues to diverse problems. One of the
677 main goals in spectral graph theory is the obtain better bounds by having access to further information on
678 the graphs.

679 For a fixed network size, the magnitude of λ_2 reflects how well connected is graph.

680 5. Stability of Synchronized Solutions

681 We will state two results on network synchronization. The first assumes that the coupling function H is
682 linear and the network is undirected. This assumption facilitates the discussion of the main ideas. Then, we

Table 1.: Network of N nodes with m mean degree. Examples of nonrandom networks are depicted in Fig. 31 and random networks in Fig. 33. For random networks, the mean degree is given by $m = \sum_k kP(k)$ where $P(k)$ is the degree distribution of the network. The randomness of the networks arises via probability p . Consider the degree distribution for the SF network $P(k) = k^{-\gamma}$. C is constant.

Network	λ_2	λ_N	k_{\max}	k_{\min}	d
complete	N	N	$N-1$	$N-1$	1
ring	$2 - 2\cos\left(\frac{2\pi}{N}\right)$	4	2	2	$\frac{(N+1)/2}{N/2}$ if N is odd if N is even
star	1	N	$N-1$	1	2
hypercube (Q_m)	2	$\frac{2\ln(N-2)}{m} \left(\frac{m}{N}\right)$	m	m	m
$2k$ -regular	$2k + 1 - \frac{\sin\left[(2k+1)\frac{\pi}{N}\right]}{\sin\left(\frac{\pi}{N}\right)}$	$2k + 1 - \frac{\sin\left[(2k+1)\frac{\pi(N-1)}{N}\right]}{\sin\left(\frac{\pi(N-1)}{N}\right)}$	$2k$	$2k$	$\frac{[(N+1)/2k]}{[N/2k]}$ if N is odd if N is even
SW network	$\sim 2k + 1 - \frac{\sin\left[(2k+1)\frac{\pi}{N}\right]}{\sin\left(\frac{\pi}{N}\right)} + Cp$	$\sim 2k + 1 - \frac{\sin\left[(2k+1)\frac{\pi(N-1)}{N}\right]}{\sin\left(\frac{\pi(N-1)}{N}\right)} + Cp$	$\sim 2k$	$\sim 2k$	$O(\log N)$
SF network	$\sim m_0 \left(1 - \frac{1}{(\gamma-1)}\right)$	$\sim m_0 N^{\frac{1}{\gamma-1}}$	$\sim m_0$	$\sim m_0 N^{\frac{1}{\gamma-1}}$	$O\left(\frac{\log N}{\log \log k}\right)$
ER network	$\sim Np$	$\sim Np$	$pN(1 + O(1))$	$(1-p)(1 + O(1))$	$\frac{\log N}{2 \log N p}$

683 will discuss the case where the coupling is nonlinear. Basically, the results are the same with an additional
 684 complication as the latter involves the theory of Lyapunov exponents.

Theorem 3: Consider the diffusively coupled network model

$$\mathbf{x}_i = \mathbf{f}(\mathbf{x}_i) - \alpha \sum_{j=1}^N L_{ij} \mathbf{H}(\mathbf{x}_j),$$

on an undirected and connected network. Assume that the \mathbf{H} is a positive definite linear operator. The reason of the assumption will appear in Step 5 of the theorem. Then, there is $\Gamma = \Gamma(\mathbf{f}, \mathbf{H})$ such that for any

$$\alpha > \frac{\Gamma}{\lambda_2},$$

the global synchronization is uniformly asymptotically stable. Moreover, the transient to the globally synchronized behavior is given the spectral gap λ_2 , that is, for any i and j

$$\|\mathbf{x}_i(t) - \mathbf{x}_j(t)\| \leq C e^{-(\alpha\lambda_2 - \Gamma)t},$$

685 where C is a constant.

686 The above result relates the threshold coupling for synchronization in contributions coming solely from
 687 dynamics Γ , and network structure λ_2 .

Definition 1 (Synchronization Threshold): We call

$$\alpha_c(\mathbf{f}, \mathbf{H}, G) = \frac{\Gamma(\mathbf{f}, \mathbf{H})}{\lambda_2(G)}$$

688 the critical synchronization coupling.

689 Therefore, for a fixed node dynamics \mathbf{f} and coupling \mathbf{H} we can analyze how distinct network facilitates
 690 or inhibits global synchronization. To continue our discussion we need the following

Definition 2 (Better Synchronizable): We say that the network G_1 is more synchronizable than G_2 if for fixed \mathbf{f} and \mathbf{H} we have

$$\alpha_c(G_1) < \alpha_c(G_2)$$

691 Likewise, we say that G_1 has better synchronizability than G_2 .

692 **5.1. Which networks synchronize best**

693 In this setting, the coupling function \mathbf{H} is positive definite and the network is undirected, the synchronizability depends only on the spectral gap. Using the previous study on the properties of various networks presented in Sec. 4.4. We consider networks of N nodes then

- 696 • A *complete graph* is the most synchronizable. In fact, $\alpha_c \approx 1/N$. So, the larger the graph the less
 697 coupling strength is necessary to synchronize the network.
- 698 • A *path* or *ring* are poorly synchronizable. For these networks, $\alpha_c \approx N^2$.
- 699 • *2k-regular graphs* share the same properties for also poorly synchronizable when $k \ll N$.
- 700 • *Erdős-Renyi graphs* the synchronization properties depend only on the mean degree $\alpha_c \approx 1 / \langle k \rangle$

- *Small world networks* are better than regular but worse than random graphs. In the limit of large graphs $\alpha_c \approx 1/s$ where s is the fraction of added random links. In general, adding links to a network favours synchronization.

704
705

706 5.2. Proof of the Stable Synchronization

707 Now we present the proof of Theorem 3. We omit some details that are not relevant for the understanding
708 of the proof. A full discussion of the proof can be found in [98]. We will show that whenever the nodes
709 start close together they tend to the same future dynamics, that is, $\|\mathbf{x}_i(t) - \mathbf{x}_j(t)\| \rightarrow 0$, for any i and j . For
710 pedagogical purposes we split the proof into five main steps.

Step 1: Kronecker Form. We have N coupled equations each has dimension n . Because of the nice structure of the interaction we can use the Kronecker product to write them as a single block. Given two matrices $\mathbf{A} \in \mathbb{R}^{p \times q}$ and $\mathbf{B} \in \mathbb{R}^{r \times s}$, the Kronecker Product of the matrices \mathbf{A} and \mathbf{B} and defined as the matrix

$$\mathbf{A} \otimes \mathbf{B} = \begin{pmatrix} A_{11}\mathbf{B} & \cdots & A_{1q}\mathbf{B} \\ \vdots & \ddots & \vdots \\ A_{p1}\mathbf{B} & \cdots & A_{pq}\mathbf{B} \end{pmatrix},$$

we introduce the following notation

$$\mathbf{X} = \text{col}(\mathbf{x}_1, \dots, \mathbf{x}_N),$$

where col denotes the vector formed by stacking the columns vectors \mathbf{x}_i into a single vector. Similarly

$$\mathbf{F}(\mathbf{X}) = \text{col}(\mathbf{f}(\mathbf{x}_1), \dots, \mathbf{f}(\mathbf{x}_N)).$$

711 Then Eq. (52) can be arranged into a compact form

$$\frac{d\mathbf{X}}{dt} = \mathbf{F}(\mathbf{X}) - \alpha(\mathbf{L} \otimes \mathbf{H})\mathbf{X}, \quad (45)$$

712 where \otimes is the Kronecker product. The easiest way to check that this is correct is to compute the i th block
713 of dimension n and compare with the equation for the i th node.

714 **Step 2: Transversal Laplacian Eigenmodes.** The Kronecker product has many nice properties such as

$$(\mathbf{A} \otimes \mathbf{B})(\mathbf{C} \otimes \mathbf{D}) = \mathbf{AC} \otimes \mathbf{BD}. \quad (46)$$

And this holds whenever the matrix multiplication make sense. A nice consequence of the multiplication result in Kronecker form is that if

$$\mathbf{A}\mathbf{v}_i = \lambda_i\mathbf{v}_i \text{ and } \mathbf{B}\mathbf{u}_j = \mu_j\mathbf{u}_j \text{ then } \mathbf{A} \otimes \mathbf{B}(\mathbf{v}_i \otimes \mathbf{u}_j) = \lambda_i\mu_j\mathbf{v}_i \otimes \mathbf{u}_j$$

715 Since we are assuming that \mathbf{L} is undirected and \mathbf{H} is positive definite the eigenvectors $\{\mathbf{v}_i\}_{i=1}^N$ of \mathbf{L} form
716 a basis of \mathbb{R}^N . Likewise, the eigenvectors of \mathbf{H} form a basis of \mathbb{R}^n . This implies that the eigenvectors of
717 $\mathbf{L} \otimes \mathbf{H}$ form a basis of \mathbb{R}^{Nn} . Using this fact we can represent \mathbf{X} as

$$\mathbf{X} = \sum_{i=1}^N \mathbf{v}_i \otimes \mathbf{y}_i$$

where \mathbf{y}_i is the coordinates of \mathbf{X} in the Kronecker basis. For sake of simplicity we call $\mathbf{y}_1 = \mathbf{s}$, and remember that $\mathbf{v}_1 = \mathbf{I}$ is an eigenvector. Hence

$$\mathbf{X} = \mathbf{I} \otimes \mathbf{s} + \mathbf{U},$$

where

$$\mathbf{U} = \sum_{i=2}^N \mathbf{v}_i \otimes \mathbf{y}_i.$$

In this way we split the contribution in the direction of the global synchronization and \mathbf{U} , which accounts for the contribution of the transversal. Note that if \mathbf{U} converges to zero then the system completely synchronizes, that is \mathbf{X} converges to $\mathbf{I} \otimes \mathbf{s}$ which clearly implies that

$$\mathbf{x}_1 = \dots = \mathbf{x}_N = \mathbf{s}$$

718 The goal then is to obtain conditions so that $\|\mathbf{U}\| \rightarrow 0$.

719
720 **Step 3: Variational equations for the Transversal Modes.** The equation of motion in terms of the
721 Laplacian modes decomposition reads

$$\mathbf{I} \otimes \frac{d\mathbf{s}}{dt} + \frac{d\mathbf{U}}{dt} = \mathbf{F}(\mathbf{I} \otimes \mathbf{s} + \mathbf{U}) - \alpha(\mathbf{L} \otimes \mathbf{H})(\mathbf{I} \otimes \mathbf{s} + \mathbf{U}),$$

We assume that \mathbf{U} is small and perform a Taylor expansion about the synchronization manifold.

$$\mathbf{F}(\mathbf{I} \otimes \mathbf{s} + \mathbf{U}) = \mathbf{F}(\mathbf{I} \otimes \mathbf{s}) + D\mathbf{F}(\mathbf{I} \otimes \mathbf{s})\mathbf{U} + \mathbf{R}(\mathbf{U}),$$

722 where $\mathbf{R}(\mathbf{U})$ is the Taylor remainder $\|\mathbf{R}(\mathbf{U})\| = O(\|\mathbf{U}\|^2)$. Using the Kronecker product properties Eq. 46
723 and the fact that $\mathbf{L}\mathbf{I} = \mathbf{0}$, together with $\mathbf{I} \otimes \frac{d\mathbf{s}}{dt} = \mathbf{F}(\mathbf{I} \otimes \mathbf{s}) = \mathbf{I} \otimes \mathbf{f}(\mathbf{s})$ and we have

$$\frac{d\mathbf{U}}{dt} = [D\mathbf{F}(\mathbf{I} \otimes \mathbf{s}) - \alpha(\mathbf{L} \otimes \mathbf{H})]\mathbf{U} + \mathbf{R}(\mathbf{U}) \quad (47)$$

724 and likewise $D\mathbf{F}(\mathbf{I} \otimes \mathbf{s})\mathbf{U} = [\mathbf{I}_N \otimes D\mathbf{f}(\mathbf{s})]\mathbf{U}$, therefore, the first variational equation for the transversal modes
725 reads

$$\frac{d\mathbf{U}}{dt} = [\mathbf{I}_N \otimes D\mathbf{f}(\mathbf{s}) - \alpha\mathbf{L} \otimes \mathbf{H}]\mathbf{U}. \quad (48)$$

726 **Step 4: Decoupling of Transversal Modes.** Instead of analyzing the full set of equations, we can do much
727 better by projecting the equation into subspace $W_i = \text{span}\{\mathbf{v}_i \otimes \mathbf{I}\}$. Let $P_i : \mathbb{R}^N \otimes \mathbb{R}^n \rightarrow W_i$ be a projection
728 operator given by $P_i = \mathbf{v}_i \mathbf{v}_i^* \otimes \mathbf{I}$, it follows that P_i is an orthogonal projection since \mathbf{v}_i 's are orthonormal.
729 Using Eq. (48) and the identity Eq. 46 we obtain

$$P_i \frac{d\mathbf{U}}{dt} = [\mathbf{v}_i \mathbf{v}_i^* \otimes D\mathbf{f}(\mathbf{s}) - \alpha(\mathbf{v}_i \mathbf{v}_i^* \otimes \mathbf{L}) \otimes \mathbf{H}]\mathbf{U}, \quad (49)$$

$$= [\mathbf{v}_i \mathbf{v}_i^* \otimes D\mathbf{f}(\mathbf{s}) - \alpha\lambda_i(\mathbf{v}_i \mathbf{v}_i^*) \otimes \mathbf{H}]\mathbf{U} \quad (50)$$

where in the last passage we used that the network is undirected implying $\mathbf{v}_i^* \mathbf{L} = \lambda_i \mathbf{v}_i^*$. Using and the fact that $\mathbf{v}_i^* \mathbf{v}_i = \delta_{ij}$, where is δ_{ij} the Kronecker delta, we have that $(\mathbf{v}_i \mathbf{v}_i^* \otimes \mathbf{I})\mathbf{U} = \sum_{j=2}^N \mathbf{v}_i \delta_{ij} \otimes \mathbf{y}_j$. Moreover, since

P_i does not depend on time $P_i \dot{\mathbf{U}} = (P_i \mathbf{U})$

$$\sum_{j=2}^N \mathbf{v}_i \delta_{ij} \otimes \frac{d\mathbf{y}_i}{dt} = \sum_{j=2}^N \mathbf{v}_i \delta_{ij} \otimes [D\mathbf{f}(\mathbf{s}) - \alpha \lambda_i \mathbf{H}] \mathbf{y}_i$$

the nonzero coefficients give the dynamics in W_i . Hence,

$$\frac{d\mathbf{y}_i}{dt} = [D\mathbf{f}(\mathbf{s}) - \alpha \lambda_i \mathbf{H}] \mathbf{y}_i$$

730 All blocks have the same form which are different only by λ_i , the i th eigenvalue of L . We can write all
731 the blocks in a parametric form

$$\frac{d\mathbf{u}}{dt} = \mathbf{K}(t)\mathbf{u}, \tag{51}$$

where

$$\mathbf{K}(t) = D\mathbf{f}(\mathbf{s}(t)) - \kappa \mathbf{H}$$

732 with $\kappa \in \mathbb{R}$. Hence if $\kappa = \alpha \lambda_i$ we have the equation for the i th block. This is just the same type of equation
733 we encounter before in the example of the two coupled oscillators, see Eq. (9).

Step 5. Stability. Because \mathbf{H} is positive definite we can first solve the homogeneous equation $\dot{\mathbf{u}} = -\kappa \mathbf{H} \mathbf{u}$. This equation has an globally attracting trivial solution. Then, we incorporate $D\mathbf{f}$ in terms of the variation of constants formula. So, first notice that

$$\mathbf{u}(t) = e^{-\kappa \mathbf{H} t} \mathbf{u}_0 \Rightarrow \|\mathbf{u}(t)\| \leq K \|\mathbf{u}_0\| e^{-\kappa \lambda_{\min}(\mathbf{H}) t}$$

where $\lambda_{\min}(\mathbf{H})$ is the smallest eigenvalue of \mathbf{H} . So, by the variation of constants formula

$$\mathbf{u}(t) = e^{-\kappa \mathbf{H} t} \mathbf{u}_0 + \int_0^t e^{-\kappa \mathbf{H}(t-\tau)} D\mathbf{f}(\mathbf{s}(\tau)) d\tau$$

taking norms

$$\|\mathbf{u}(t)\| = K \|\mathbf{u}_0\| + \int_0^t e^{-\kappa \lambda_{\min}(\mathbf{H})(t-\tau)} \|D\mathbf{f}(\mathbf{s}(\tau))\| d\tau$$

where K is a constant and defining $M_f = \sup_t \|D\mathbf{f}(\mathbf{s}(t))\|$ by Gronwal inequality

$$\|\mathbf{u}(t)\| = K_1 \|\mathbf{u}_0\| e^{(-\kappa \lambda_{\min}(\mathbf{H}) + M_f)t}.$$

The trivial solution will be exponentially stable when

$$-\kappa \lambda_{\min}(\mathbf{H}) + M_f < 0 \Rightarrow \kappa > \Gamma = \frac{M_f}{\lambda_{\min}(\mathbf{H})}$$

Recall that taking $\kappa = \alpha \lambda_i > \Gamma$ we are stabilizing the equation for the i th block. But, once we stabilize the second block all blocks will be stable (because λ_2 is the smallest nonzero eigenvalue)

$$\alpha \lambda_N \geq \dots \geq \alpha \lambda_3 \geq \alpha \lambda_2 \geq \Gamma$$

Hence, the stability condition so that all blocks have exponentially stable trivial solution is

$$\alpha > \frac{\Gamma}{\lambda_2}$$

734 Using the bounds for the blocks it is easy to obtain a bound for the norm of the evolution operator. Indeed,
735 in view of the previous estimates, we note that

$$\begin{aligned} \|\mathbf{U}(t)\|_2 &\leq \sum_{i=2}^N K_i \|\mathbf{v}_i\| \|\mathbf{y}_i(s)\| e^{-(\alpha\lambda_i - \Gamma)(t-s)} \\ &\leq K_2 e^{-\eta(t-s)} \end{aligned}$$

736 with $\eta = \alpha\lambda_2 - \Gamma$ for any $t \geq s$.

Because the trivial solution is exponentially stable (uniformly in $s(t)$) by the principle of linearization, we conclude that the nonlinearities coming Taylor remainder does not affect the stability of the trivial solution, which correspond to the global synchronization. The claim about the transient is straightforward, because all norms are equivalent in finite dimensions we can take

$$\|\mathbf{X}(t) - \mathbf{I} \otimes \mathbf{s}(t)\|_\infty \leq K_3 e^{-\eta(t-s)} \|\mathbf{U}(s)\|_\infty$$

implying that $\max_i \|\mathbf{x}_i(t) - \mathbf{s}(t)\|_2 \leq K_3 e^{-\eta(t-s)} \|\mathbf{U}(s)\|_\infty$ and in virtue of the triangular inequality

$$\|\mathbf{x}_i(t) - \mathbf{x}_j(t)\|_\infty \leq \|\mathbf{x}_i(t) - \mathbf{s}(t)\|_\infty + \|\mathbf{x}_j(t) - \mathbf{s}(t)\|_\infty$$

737 and using the previous bound, we concluding the proof. \square

738 6. General Diffusive Coupling and Master Stability Function

Until now we have considered linear coupling functions which are positive definite. This assumption can be relaxed and thereby we are generalize our previous results. The statement will then become rather technical and will be beyond the scope of our review. So, here we will discuss the main ideas but will not give much details on the technical issues. Consider the function $\mathbf{g} : \mathbb{R}^m \times \mathbb{R}^n \rightarrow \mathbb{R}^n$. We say that \mathbf{g} is diffusive if

$$\mathbf{g}(\mathbf{x}, \mathbf{x}) = 0 \text{ and } \mathbf{g}(\mathbf{x}, \mathbf{y}) = -\mathbf{g}(\mathbf{y}, \mathbf{x})$$

739 Hence, we can extend the model to a general diffusive coupling

$$\dot{\mathbf{x}}_i = \mathbf{f}(\mathbf{x}_i) + \alpha \sum_{j=1}^N A_{ij} \mathbf{g}(\mathbf{x}_j, \mathbf{x}_i). \tag{52}$$

We perform the analysis close to synchronization $\mathbf{x}_i = \mathbf{s} + \xi_i$ so

$$\mathbf{g}(\mathbf{x}_j, \mathbf{x}_i) = \mathbf{g}(\mathbf{s} + \xi_j, \mathbf{s} + \xi_i) = \mathbf{g}(\mathbf{s}, \mathbf{s}) + D_1 \mathbf{g}(\mathbf{s}, \mathbf{s}) \xi_j + D_2 \mathbf{g}(\mathbf{s}, \mathbf{s}) \xi_i$$

but because the coupling is diffusive

$$D_2 \mathbf{g}(\mathbf{s}, \mathbf{s}) = -D_1 \mathbf{g}(\mathbf{s}, \mathbf{s})$$

we obtain

$$\mathbf{g}(\mathbf{x}_j, \mathbf{x}_i) = \mathbf{G}(s)(\xi_j - \xi_i) + \mathbf{R}(\xi_i, \xi_j)$$

740 where $\mathbf{G}(s) = D_1\mathbf{g}(s, s)$ and $\mathbf{R}(\xi_i, \xi_j)$ contains quadratic terms. So, the first variational equation about the
 741 synchronization manifold

$$\dot{\xi}_i = D\mathbf{f}(s(t))\xi_i + \alpha \sum_{j=1}^N A_{ij}\mathbf{G}(s)(\xi_j - \xi_i) \quad (53)$$

$$= D\mathbf{f}(s(t))\xi_i - \alpha\mathbf{G}(s) \sum_{j=1}^N L_{ij}\xi_j. \quad (54)$$

Now we can perform the same steps as before. In fact, Steps 1 – 4 remain unchanged. The change difference is Step 5, which concerns the stability of the modes. Performing all the steps 1 to 4 we obtain the parametric equation for the modes

$$\dot{\mathbf{u}} = [D\mathbf{f}(s(t)) - \kappa\mathbf{G}(s(t))]\mathbf{u}$$

742 And we can no longer apply the *trick* of using the coupling function \mathbf{H} to solve the equation. Here, $\mathbf{G}(s(t))$
 743 depends on time and this generality tackling the stability of the trivial solution is challenging.

The main idea is to fix κ compute the maximum Lyapunov exponent $\Lambda(\kappa)$ as

$$\|\mathbf{u}(t)\| \leq Ce^{\Lambda(\kappa)t}$$

744 see Appendix B. The map

$$\kappa \mapsto \Lambda(\kappa) \quad (55)$$

745 is called Master Stability Function. Notice that if $\Lambda(\kappa) < 0$ when $\kappa \in (\alpha_c^1, \alpha_c^2)$ then $\|\mathbf{u}\| \rightarrow 0$.
 The stability condition then become

$$\alpha_c^1 \leq \alpha\lambda_2 \leq \dots \leq \alpha\lambda_N \leq \alpha_c^2$$

746 Or

$$\frac{\alpha_c^2}{\alpha_c^1} \geq \frac{\lambda_N}{\lambda_2} \quad (56)$$

747 This is a well studied condition. Much energy has been devoted to study the master stability function Eq.
 748 55, see e.g., [53, 113].

749 **6.1. Examples of Master Stability Functions**

Now let us consider coupled Rössler systems which are coupled through their x -coordinates:

$$\begin{aligned} \dot{x}_i &= -y_i - z_i + \alpha \sum_{j=1}^N A_{ij}(x_j - x_i) \\ \dot{y}_i &= x_i + ay_i \\ \dot{z}_i &= b + z_i(x_i - c) . \end{aligned} \tag{57}$$

750 In order to compute $\Lambda_{\max}(\kappa)$, we find that Df and DH are given by

$$Df(s) = \begin{pmatrix} 0 & -1 & -1 \\ 1 & a & 0 \\ z^* & 0 & x^* - c \end{pmatrix} \quad \text{and} \quad DH = H = \begin{pmatrix} 1 & 0 & 0 \\ 0 & 0 & 0 \\ 0 & 0 & 0 \end{pmatrix} , \tag{58}$$

751 x and z are the components of s . The constants are $a = 0.2$, $b = 0.2$ and $c = 5.7$.

752 To compute $\Lambda(\kappa)$, we first simulate the isolated dynamics $\dot{s} = f(s)$ and obtain the trajectory $s(t)$, then we
 753 feed this trajectory to $\dot{u} = [Df(s(t)) - \kappa H]u$ and then for each κ estimate the maximal Lyapunov exponent $\Lambda(\kappa)$. The result is depicted in Fig. 35.

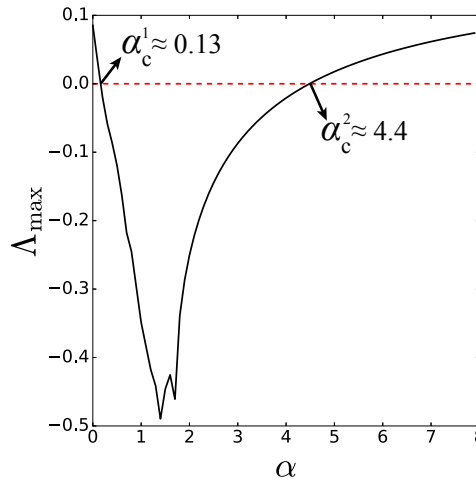


Figure 35.: Master stability function for x -coupled Rössler attractors on a network structure.

754 Stability region where Λ is negative is bounded between $\alpha_c^1 \approx 0.13$ and $\alpha_c^2 \approx 4.4$. So, if the network is a complete graph then $\lambda_2 = \dots = \lambda_N = N$, so the network synchronization when

$$\frac{\alpha_c^2}{N} > \alpha > \frac{\alpha_c^1}{N}$$

755 **6.2. Synchronization conditions and Synchronization Loss**

756 In Sec .5.1, we discussed the synchronizability of network types when there is only one critical threshold
 757 in other words $\alpha_c^2 \rightarrow \infty$. This case is true when H is a positive matrix. In the general case, there are two
 758 finite critical couplings Eq. 56 and the master stability function has a finite stability region between these
 759 critical points (as discussed in the above section). Now we discuss this synchronization scenario for various
 760 network types. To quantify the synchronizability, we will use the network properties given in Table. 1.

761 **2k-regular graphs – Diameter driven synchronization loss.** When $k \ll N$, the mean geodesic distance
 762 (shortest path length) between nodes are increasing very fast as N increasing. Hence, while the di-
 763 ameter of the network is increasing $d = 2N/k$, speed of information exchange between the nodes is
 764 decreasing drastically. In this case, the complete synchronization is not stable and it is visible from
 765 the Laplacian spectrum of the graph. For $N \rightarrow \infty$ and $k \ll N$, the extremal eigenvalues given in Table 1
 766 can be extended to Taylor expansion and major role playing part can be rewritten as

$$\lambda_2 = \frac{4\pi^2(k + \frac{1}{2})^3}{3N^2} \text{ and } \lambda_N = 2k \frac{N}{N-1}$$

The ratio between the largest λ_N and second smallest eigenvalue λ_2 of the Laplacian is not growing in the same scale,

$$\frac{\lambda_N}{\lambda_2} \approx N^2/k^2$$

767 and the condition in Eq. (56) is never satisfied.

768 **ER graphs – Optimal Synchronization.** In this case, the extremal eigenvalues λ_2 and λ_N of the Laplacian
 769 matrix increase in the same scale. The diameter of the network increases very slowly $d \approx \log N$ when
 770 the network size N increases Table 1. Therefore the synchronization is stable for any scale of size.

771 **BA networks – Heterogeneity driven synchronization loss.** When the network is too heterogeneous the
 772 complete synchronization is unstable, this is because the extremal eigenvalues λ_2 and λ_N grow in
 773 different scales and the condition in Eq. (56) is never met. For instance, consider a BA network.
 774 Then, the eigenvalues satisfy

$$\lambda_2 \approx m_0 \text{ and } \lambda_N \approx m_0 N^{1/2}$$

775 where m_0 is the mean degree. Hence, the eigenratio becomes

$$\frac{\lambda_N}{\lambda_2} \approx N^{1/2}$$

this should be compared to the stability interval given by the master stability function. Lets consider the example in the above section with the Rössler Eq. (58). The master stability function gives (as seen in Figure 35) an stability interval $\alpha_c^2/\alpha_c^1 \approx 34$. The stability conditions Eq. (56) reads as

$$N^{1/2} < 34$$

So, when the BA network is large enough it is not possible to synchronize the system. In particular the critical system size to be able to synchronization a network of Rössler as in Eq. (58) is, therefore,

$$N \approx 10^3.$$

776 6.2.1. Extensions

777 There are a few extensions of the model. Here we discuss a few directions.

778 **Directed Networks.** The major problem considering directed networks is that they may not be diagonal-
 779 izable. So, the decoupling of transversal modes by projection is a nontrivial steps. There are a few
 780 ways to overcome this. The first, using Jordan decomposition of the Laplacian. The other possibility
 781 is to perturb the Laplacian to make the eigenvalues simples. This must be done in such a way that

782 the perturbation does not spoil the stability. In both cases, the stability condition remain unchanged.
 783 Only the transients may be longer.

784 When the network is nondiagonalizable, small perturbations in the network may lead to large
 785 perturbations in the eigenvalues (the eigenvalues in this case are not differentiable functions of the
 786 perturbations) [81]. Moreover, structural improvements in the network may lead to desynchronization
 787 [85].

Nonidentical Nodes Here we consider $f(\mathbf{x}) \mapsto f(\mathbf{x}) + \mathbf{r}_i(\mathbf{x}, t)$, where \mathbf{r}_i is either a perturbation of the vector field or a signal playing the role of noise. When \mathbf{r}_i is very small synchronization will persist [15]. For general networks, Bollt and co-workers [127] extended the master stability function approach when \mathbf{r}_i is a perturbation of the vector field. Pereira and co-workers [99] study the effect of general perturbations $\|\mathbf{r}_i\| \leq \delta$ and the role that the network structure plays in suppressing the fluctuations. In the case where \mathbf{H} is positive definite and the network is undirected, they showed that the synchronization error

$$E = \frac{1}{n(n-1)} \sum_{ij} \|\mathbf{x}_i - \mathbf{x}_j\|$$

behaves as

$$E \leq K \frac{\delta}{\alpha \lambda_2 - \alpha_c}$$

788 For example, if the oscillators were uncoupled and \mathbf{r}_i independent noise then the Central Limit
 789 theorem would yield $E = O(N^{-1/2})$. For complete networks, the interaction and synchronization
 790 yields $E = O(N^{-1})$ which is a large improvement over the naive application of the Central Limit
 791 theorem. In certain sense, this shows that interacting maybe better then isolation.

Nonidentical Coupling Functions In many applications the coupling function are not identical and has fluctuating components [69, 121]. Consider an undirected networks of identical oscillators and coupling function

$$\mathbf{H}_{ij}(\mathbf{x}_i - \mathbf{x}_j, t) = \mathbf{H}_{ij}(\mathbf{x}_i - \mathbf{x}_j) + \mathbf{P}_{ij}(\mathbf{x}_i - \mathbf{x}_j, t)$$

792 where $\|\mathbf{P}_{ij}(\mathbf{x}_i - \mathbf{x}_j, t)\| \leq \eta$. In this case, the network structure will play a major on the size of per-
 793 turbation η . If the network is random and the degree distribution homogeneous, then even for large
 794 perturbations δ synchronization is stable. If the network is heterogeneous degrees such as Barabasi-
 795 Albert then typically $\delta_c = O(N^{-\beta})$ is the critical perturbation size. If $\delta > \delta_c$ synchronization becomes
 796 unstable, solely because of the interaction between network structure and perturbations in the cou-
 797 pling function.

798 **Cluster Synchronization** According to similarities in coupled systems, such as symmetries in network
 799 topology or identical dynamics in a diverse population or equally time-delayed nodes in differently
 800 distributed feedbacks, the partial or cluster synchronization can emerge. In order to enlighten the
 801 reason of these cluster synchronization cases, many techniques are developed and experimental ob-
 802 servations are analyzed[18, 28, 37, 117, 125, 133, 140].

803 The symmetries are easy to detect for some network geometries for instance Bethe lattice is a
 804 regular graph which grows from a root (parent) node by p -nodes for ℓ -levels, an example of Bethe
 805 lattice given in Fig. 36 for $p = 3$ and $\ell = 3$. The nodes in the same level of the Bethe graph, they all
 806 symmetric to each other. In Fig. 36, the levels of the graph are given in the same color and the cluster
 807 synchronization occurs for each level.

808 Recently, Pecora *et al.* put forward that all the symmetries in network structures are not visible di-
 809 rectly. They developed a computational group theory based method to reveal these hidden symmetries
 810 and predicted possible synchronization patterns [93, 118].

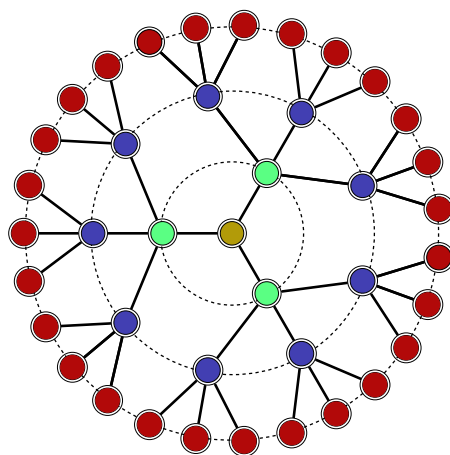


Figure 36.: Bethe lattice graph: an example of symmetries in network structure. Nodes in the same level of the Bethe graph are exactly symmetric to each other. Therefore same color nodes constitute a cluster.

811 **Time Delay Coupling** Simultaneous coupling is not always possible for real world applications in other
 812 words some time delays can occur in the interaction process. Therefore it is important to investigate
 813 synchronizability and stability of coupled time-delayed systems. The necessary conditions for time
 814 delayed synchronization is analytically shown by Pyragas [104]. The finding of time-delay synchrono-
 815 nization is used as an application for the anticipating synchronization (see Section 3.4).

816 7. Conclusions

817 In this article, we have surveyed the phenomenon of synchronization in coupled chaotic dynamical systems
 818 and some of its applications. Synchronization of chaos may be a counter-intuitive surprise at first sight.
 819 From where does coherence arise through coupling for chaotic systems, the trajectories of which are sen-
 820 sitive to initial conditions and diverge from each exponentially fast? We have discussed basic results for
 821 synchronization of two coupled chaotic systems and more advanced ones concerning synchronization in
 822 complex networks, as well as various applications.

823 In Sec. 2, we have started discussing synchronisation of coupled linear systems. Even though it is el-
 824 elementary and straightforward, this example harbors the principal ideas behind synchronization and we
 825 presented all carefully in all mathematical detail. In the setting of two coupled nonlinear systems, three
 826 types of synchronization have been identified: complete, phase and generalized synchronization.

827 In Sec. 3 we have proceeded to discuss applications of all of these types of synchronization: secure com-
 828 munication by complete and phase synchronization, parameter estimation and prediction by generalized
 829 synchronization and anticipation by complete synchronization in delayed systems.

830 In Sec. 4 synchronization on complex networks has been discussed with a focus on diffusively interacted
 831 chaotic oscillator networks, since such models are relevant to problems of interest, such as neural networks
 832 in the brain, arrays of coupled lasers and interacting pacemaker cells.

833 In Sec. 5, stability results from the theory of nonautonomous differential equation have been used to
 834 establish conditions for stable global synchronization in networks of diffusively linearly coupled dissipa-
 835 tive dynamical systems. There are two microscopic conditions concerning the isolated dynamics and one
 836 macroscopic condition in terms of eigenvalues of the Laplacian matrix of the network. Stable synchrono-
 837 nization is important and our detailed and rigorous discussion of the stability of synchronization cannot be
 838 found elsewhere in the literature. Stability conditions for general coupling functions and master stability
 839 function have been analyzed in Sec. 6.

840 Synchronization remains a topic of active research. Many important questions remain open, such as
841 putting the theory phase synchronization on a solid mathematical foundation. Section 6.2.1 discusses topi-
842 cal research questions. We hope to have succeeded preparing the reader to appreciate some of the challenges
843 and opportunities in this exciting field of research and a basis to contribute to future developments.

844 **Acknowledgements**

845 We are grateful to the Nesin Maths Village (Turkey) for the stimulating atmosphere and hospitality during
846 a visit where part of this paper was written. This work was supported by the European Research Coun-
847 cil [ERC AdG grant number 339523 RGDD]; EU Horizon2020 Innovative Training Network CRITICS
848 [grant number 643073]; a FAPESP-Imperial College SPRINT grant under FAPESP Cemeai [grant number
849 2013/07375-0], and Russian Science Foundation [grant number 14-41-00044] at the Lobayevsky University
850 of Nizhny Novgorod.

851 **Appendix A. List of frequently used notions and abbreviations**

852 ***Table of notions***

	$ \cdot $	absolute value
	$\ \cdot\ $	norm
	δ_{ij}	Kroneker delta
	G	graph
	L	Laplacian matrix
	A	adjacency matrix
	I	identity matrix
	H	coupling function
	$\mathbf{1}$	vector whose every components is 1
	α	coupling strength
	α_c	critical coupling strength for synchronization
	f	isolated dynamics (vector field)
853	Λ	Maximum Lyapunov exponent
	λ_2	spectral gap: the second minimum eigenvalue of Laplacian matrix
	Df	Jacobian matrix of f
	ϕ	phase
	t	time
	a, b and c	parameters of Rössler system
	σ, ρ and β	parameters of Lorenz system
	n	dimension of vector fields
	i and j	natural numbers
	N	system size of networks
	M	total number of links
	k_i	degree of i -th node
	d	diameter of a network

854 ***Table of abbreviations***

	CS	complete synchronization
	PS	phase synchronization
	GS	generalized synchronization
	AS	anticipating synchronization
855	ER	Erdős - Renyi network
	SF	Scale-free network
	SW	Small world network
	BA	Barabasi - Albert network

856 **Appendix B. Lyapunov exponent**

857 Sensitive dependence on initial conditions is one of the main characteristics of chaotic systems. The main
 858 idea is that nearby orbits diverge at an exponential rate. This rate is called Lyapunov exponents. In this
 859 Appendix, we provide the basic notions on the theory of Lyapunov exponents.

860 If we have a nonlinear equation we can study the properties of a given solution s by linearizing the
 861 dynamics around the orbit, as we have done in Sec 2.2. This procedure leads to a linear nonautonomous
 862 equation

$$\mathbf{v}' = \mathbf{A}(t) \mathbf{v}$$

863 where \mathbf{A} is continuous and bounded matrix function. The goal is to study the behaviour of solutions. Typ-
 864 ically solving the equation explicitly is impossible. So the theory of Lyapunov exponents plays a major
 865 role.

866 Let $\mathbf{v} : \mathbb{R} \rightarrow \mathbb{R}^n$ be a solution $\mathbf{v}' = \mathbf{A}(t) \mathbf{v}$ and $\mathbf{T}(t, s)$ is the fundamental matrix. The Lyapunov exponent
 867 of the solution is defined as

$$\lambda(\mathbf{v}) = \overline{\lim}_{t \rightarrow \infty} \frac{1}{t} \ln \|\mathbf{T}(t, s) \mathbf{v}(s)\|$$

868 We also define $\lambda(0) = -\infty$. The largest Lyapunov exponents is our main object of study and is given by

$$\Lambda = \overline{\lim}_{t \rightarrow \infty} \frac{1}{t} \ln \|\Pi(t, s)\|.$$

869 The maximum Lyapunov exponent Λ determines the behaviour of solutions asymptotically because

$$\|\mathbf{v}(t)\| < C_\epsilon e^{(\Lambda + \epsilon)t}$$

870 If $\Lambda < 0$, the trivial solution $\mathbf{v}(t) = 0$ is asymptotically stable. Lyapunov exponents generalizes stability
 871 criteria for autonomous (given by eigenvalues) and periodic equations (given by Floquet exponents).

872 **Lemma B.1:** Let $\mathbf{A} \in \text{Mat}(n)$ and \mathbf{v} be an eigenvector of $\mathbf{A}\mathbf{v} = \beta\mathbf{v}$. Then $\lambda(\mathbf{v}) = \beta$.

873 If all $\lambda(\mathbf{v}) < 0$, we have $\max_{\mathbf{v}} \{\lambda(\mathbf{v})\} = \Lambda < 0$, and the trivial solution is asymptotically stable. The
 874 Lyapunov exponent also generalizes the Floquet exponents.

875 **Lemma B.2:** Let $\mathbf{A}(t)$ be a periodic matrix by the Floquet representation we have $\mathbf{T}(t, s) =$
 876 $\mathbf{P}(t, s)e^{(t-s)\mathbf{Q}(s)}$. Let \mathbf{v} be an eigenvector of $\mathbf{Q}(s)$, then $\lambda(\mathbf{v})$ is an eigenvalue of $\mathbf{Q}(s)$.

877 Hence, Lyapunov exponents are the eigenvalues of the monodromy matrix \mathbf{Q} . Although, for the synchro-
 878 nization analysis we care about the maximal Lyapunov exponents, it is important to know that there are at
 879 most n distinct Lyapunov exponents because the set $X = \{\mathbf{v}(t) | \lambda(\mathbf{v}) \leq \alpha\}$ is a vector space.

880 Appendix C. Lyapunov Function

881 One of the main techniques to tackle stability of nonlinear system is the Lyapunov function method. The
 882 method by Lyapunov allows us to obtain the stability without finding the trajectories by studying properties
 883 of the Lyapunov function. We consider a dynamical system is modelled by a differential equation

$$\dot{\mathbf{x}} = \frac{d\mathbf{x}}{dt} = \mathbf{f}(\mathbf{x}) \tag{C1}$$

We will study notions relative to connected nonempty subsets Ω of \mathbb{R}^m . A function $V : \mathbb{R}^m \rightarrow \mathbb{R}$ is said to be positive definite with respect to the set B if $V(\mathbf{x}) > 0$ for all $\mathbf{x} \in \mathbb{R}^q \setminus \Omega$. It is radially unbounded if

$$\lim_{\|\mathbf{x}\| \rightarrow \infty} V(\mathbf{x}) = \infty.$$

Note that this condition guarantees that all level sets of V are bounded. This fact plays a central role in the analysis. We also define $V' : \mathbb{R}^m \rightarrow \mathbb{R}$ as

$$V'(\mathbf{x}) = \nabla V(\mathbf{x}) \cdot \mathbf{f}(\mathbf{x}).$$

where \cdot denotes the Euclidean inner product. This definition agrees with the time derivative along the trajectories. That is, if $\mathbf{x}(t)$ is a solution of Eq. (C1), then by the chain rule

$$V'(\mathbf{x}(t)) = \nabla V(\mathbf{x}(t)) \cdot \mathbf{f}(\mathbf{x}(t))$$

884 This has a nice geometric interpretation. Since $\nabla V(\mathbf{x}(t))$ is perpendicular to the level set of V if $V'(\mathbf{x}(t)) < 0$
 885 it means that the vector field is point inwards the level set and trajectories will enter the level set and never
 886 leave it. Repeating the argument we obtain stability as the following statement shows

Theorem 4 (Lyapunov): Let $V : \mathbb{R}^n \rightarrow \mathbb{R}$ be radially unbounded and positive definite with respect to the set $\Omega \subset D$. Assume that

$$V'(\mathbf{x}) < 0 \text{ for all } \mathbf{x} \in \mathbb{R}^n \setminus \Omega$$

887 Then all trajectories of Eq. (C1) eventually enter the set Ω , in other words, the system is dissipative.

888 There are also converse Lyapunov theorems [68]. Typically if the system is dissipative (and have nice
 889 properties) then there exists a Lyapunov function.

890 Appendix D. Chaos in Lorenz system

891 In order to understand the behaviour of a continuous system, we can use the concept of a Poincaré section
 892 – a transversal surface to the flow. This method was developed by Henri Poincaré in 1890s. The crossing
 893 points are a set of discrete numbers and this number sequence is called Poincaré map. We can study the
 894 structure of the crossings of the trajectory to the surface. This reduces the dimension of the system by 1. The
 895 structure of crossing points between the plane and the trajectory determines the behaviour of the system.
 896 For example, if the trajectory cross the section always at same k -coordinate points and repeat these points
 897 in the same order then the system is periodic so-called period- k .

898 The maxima of z -component of the Lorenz system, which is Poincaré section of velocities, graphically
 899 show the chaotic regime clearly. The governing equation of the Poincaré map ($\{z_n\}$) can be plotted as z_n vs
 900 z_{n+1} (Fig. D1 (a)) which resembles the tent map function (Fig. D1 (b)). The tent map is given by

$$f(x_n) = x_{n+1} = \begin{cases} 2x_n & 0 \leq x_n \leq 1/2 \\ 2 - 2x_n & 1/2 < x_n \leq 1. \end{cases}$$

901 Lyapunov exponent of the tent map

$$\Lambda = \lim_{t \rightarrow \infty} \frac{1}{t} \ln \|Df(x)\| \tag{D1}$$

902 where Df is the Jacobian of f and $\|Df(x)\| = 2$ for all $x \neq 1/2$ since the function is not differentiable at
 903 $x = 1/2$. Therefore the Lyapunov exponent is $\Lambda = \ln 2$ and according to the positive Lyapunov exponent,
 904 the behaviour of the system is chaotic.

905 The definition of chaos given by Devaney is the the following let X be a metric space and a continuous
 906 map $f : X \rightarrow X$ is chaotic if

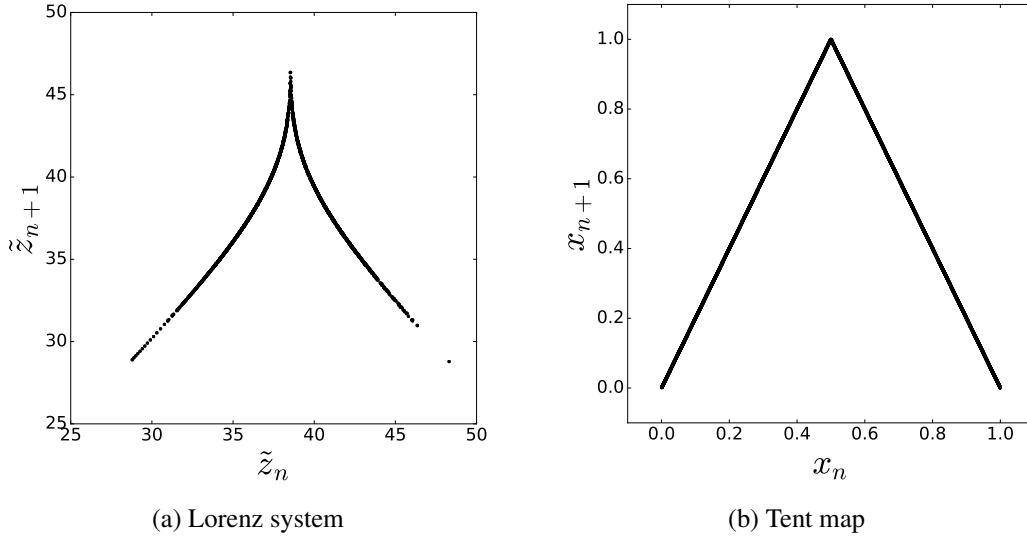


Figure D1.: Similarity between Poincaré map of Lorenz system and the tent map.

- 907 (1) f is transitive (indecomposability); that is any non-empty intervals $U, V \subset X$ there exist a natural
 908 number k such that $f^k(U) \cap V$. The transitivity condition means that X cannot be split into two open
 909 invariant sets.
- 910 (2) the periodic trajectories of f are dense in X . So, a subset contains infinitely many periodic points.
- 911 (3) f has sensitive dependence on initial conditions (unpredictability); that is if there is an infinitesimal
 912 distance δ_0 between any two point $x, y \in X$ and there exists a nonnegative number k such that after
 913 n iterations the distance between $f^n(x)$ and $f^n(y)$ is larger than $\delta_n > \delta_0$. These nearly started orbits
 914 diverge from each other at a rate Λ (see Appendix B).
 915 More details can be found in the reference [49].

916 **Appendix E. Mathematical Structure of Generalized Synchronization**

For completeness, we include this brief discussion of the mathematical structure of GS and it may be skipped without harm to the remaining sections. Again lets consider the $\psi : \mathbb{R}^m \rightarrow \mathbb{R}^n$ and the manifold

$$M = \{(\mathbf{x}, \mathbf{y}) \in \mathbb{R}^n \times \mathbb{R}^m : \mathbf{y} = \psi(\mathbf{x})\} \subset \mathbb{R}^{n+m}.$$

917 GS corresponds to the case where M is normally attracting. Lets review the notion of normally attracting
 918 invariant manifold (NAIM). M is normally attracting if it is invariant under the flow Φ (of the full system)
 919 and the dynamics in the directions normal to M is contracting stronger than in direction tangential to M .
 920 If M is a NAIM for the system F . Then there exist locally invariant stable manifolds $W_{loc}^s(M)$ such that
 921 $W_{loc}^s(M)$ is tangent to $TM \oplus E_s$ at M and $W_s(M) \in C^r$. Moreover, $W_{loc}^s(M)$ consists of all points near M
 922 whose forward orbit converges to M at rate $e^{-\eta t}$. For each $\mathbf{y} \in W_s(M)$ shadows a point $\mathbf{x} \in M$ such that
 923 $\mathbf{y} \in W_{loc}^s(\mathbf{x})$ and

$$\|\Phi^t(\mathbf{y}) - \Phi^t(\mathbf{x})\| \leq C e^{-\eta t} \|\mathbf{y} - \mathbf{x}\| \tag{E1}$$

Since the orbits of points $\mathbf{x}_0, \mathbf{x}_1 \in M$ cannot approach each other that fast, we can characterize points $\mathbf{y} \in W_{loc}^s(\mathbf{x})$ precisely as those that satisfy Eq. (E1). Lets consider consider the straitening of the manifold.

That is, we introduce new coordinates

$$\mathbf{u} = \mathbf{y} - \boldsymbol{\psi}(\mathbf{x})$$

in this coordinates the manifold corresponds to the x axis and u are the normal directions to M . Lets take two points $\mathbf{u}_1, \mathbf{u}_0 \in W_{loc}^s(\mathbf{x})$ then

$$\mathbf{u}_i = \mathbf{y}_i - \boldsymbol{\psi}(\mathbf{x}) \Rightarrow \mathbf{u}_1 - \mathbf{u}_0 = \mathbf{y}_1 - \mathbf{y}_0$$

Hence, if

$$\|\mathbf{y}_1 - \mathbf{y}_0\| \leq Ke^{-\eta t}$$

924 and η is larger than the smallest Lyapunov exponents of the driver in modulus the manifold M will be
 925 normally attracting, according to condition (3). In fact, $\boldsymbol{\psi}$ will be differentiable. Another important fact to
 926 the mention is that NAIM persist under small perturbations. For us this means that once we obtain GS small
 927 perturbations such as increasing the coupling strength will be destroy GS [34, 35]. If the condition is not
 928 satisfied then $\boldsymbol{\psi}$ won't be a NAIM. However, it may still happen that when $r = 0$ and M is attracting. In this
 929 case, $\boldsymbol{\psi}$ is only continuous. This is called strong and weak generalized synchronization [54].

Back to our Diffusively driven oscillator. In Sec. 2.4.1 we showed the contraction rate between two nearby trajectories is

$$\eta = \alpha \lambda_{min} - \|D\mathbf{g}\|$$

On the other hand, the smallest Lyapunov exponent of the driver is at most $-\|D\mathbf{f}\|$, hence the condition for normal attraction is

$$\eta > \|D\mathbf{f}\| \Rightarrow \alpha > \frac{\|D\mathbf{f}\| + \|D\mathbf{g}\|}{\lambda_{min}}$$

930 This gives the bound for M to be NAIM.

931 References

- 932 [1] Abarbanel, H. D. I., Rulkov, N. F., and Sushchik, M. M. (1996). Generalized synchronization of chaos: The
 933 auxiliary system approach. *Physical Review E*, 53(5):4528–4535.
- 934 [2] Afraimovich, V. S., Verichev, N. N., and Rabinovich, M. I. (1986). Stochastic synchronization of oscillation in
 935 dissipative systems. *Izvestiya Vysshikh Uchebnykh Zavedenii, Radiofizika*, 29(9):795–803.
- 936 [3] Albert, R. and Barabási, A.-L. (2002). Statistical mechanics of complex networks. *Reviews of Modern Physics*,
 937 74(January):48–94.
- 938 [4] Albert, R., Jeong, H., and Barabási, A.-L. (2000). Error and attack tolerance of complex networks. *Nature*,
 939 406(July):378–381.
- 940 [5] Anishchenko, V. S., Vadivasova, T. E., Postnov, D. E., and Safonova, M. A. (1992). Synchronization of Chaos.
 941 *International Journal of Bifurcation and Chaos*, 2(3):633–644.
- 942 [6] Arenas, A., Díaz-Guilera, A., Kurths, J., Moreno, Y., and Zhou, C. (2008). Synchronization in complex networks.
 943 *Physics Reports*, 469(3):93–153.
- 944 [7] Ashwin, P., Buescu, J., and Stewart, I. (1994). Bubbling of attractors and synchronisation of chaotic oscillators.
 945 *Physics Letters A*, 193(2):126–139.
- 946 [8] Ashwin, P., Terry, J. R., Thornburg, K. S., and Roy, R. (1998). Blowout bifurcation in a system of coupled chaotic
 947 lasers. *Physical Review E*, 58(6):7186–7189.
- 948 [9] Balanov, A., Janson, N., Postnov, D., and Sosnovtseva, O. (2009). *Synchronization: From Simple to Complex*.
 949 Springer-Verlag Berlin Heidelberg.

- 950 [10] Baptista, M. S., Pereira, T., and Kurths, J. (2006). Upper bounds in phase synchronous weak coherent chaotic
951 attractors. *Physica D*, 216(2):260–268.
- 952 [11] Baptista, M. S., Pereira, T., Sartorelli, J. C., Caldas, I. L., and Kurths, J. (2005). Non-transitive maps in phase
953 synchronization. *Physica D*, 212(3-4):216–232.
- 954 [12] Baptista, M. S., Silva, T. P., Sartorelli, J. C., Caldas, I. L., and Rosa, E. (2003). Phase synchronization in the
955 perturbed Chua circuit. *Physical Review E*, 67:056212.
- 956 [13] Barabási, A.-L. and Albert, R. (1999). Emergence of Scaling in Random Networks. *Science*, 286(October):509–
957 512.
- 958 [14] Barahona, M. and Pecora, L. M. (2002). Synchronization in Small-World Systems. *Physical Review Letters*,
959 89(5):054101 (1–4).
- 960 [15] Belykh, I., Belykh, V., Nevidin, K., and Hasler, M. (2003). Persistent clusters in lattices of coupled nonidentical
961 chaotic systems. *Chaos*, 13(1):165–178.
- 962 [16] Belykh, I., De Lange, E., and Hasler, M. (2005). Synchronization of bursting neurons: What matters in the
963 network topology. *Physical Review Letters*, 94(18):1–4.
- 964 [17] Belykh, I., Jeter, R., and Belykh, V. (2016). Foot force models of crowd dynamics on a wobbly bridge.
965 *arXiv:1610.05366v1*, pages 1–15.
- 966 [18] Belykh, V. N., Osipov, G. V., Petrov, V. S., Suykens, J. A. K., and Vandewalle, J. (2008). Cluster synchronization
967 in oscillatory networks. *Chaos*, 18(3):037106 (1–6).
- 968 [19] Bode, N. W. F., Faria, J. J., Franks, D. W., Krause, J., and Wood, a. J. (2010). How perceived threat increases
969 synchronization in collectively moving animal groups. *Proc. R. Soc. B*, 277(1697):3065–70.
- 970 [20] Bollobás, B. (1998). *Modern Graph Theory*. Springer-Verlag New York.
- 971 [21] Carroll, T. L., Heagy, J., and Pecora, L. M. (1996). Transforming signals with chaotic synchronization. *Physical
972 Review E*, 54(5):4676–4680.
- 973 [22] Carroll, T. L. and Pecora, L. M. (1998). Synchronizing Hyperchaotic Volume-Preserving Maps and Circuits.
974 *IEEE Trans. Circuits Syst., I: Fund. Theory and App*, 45(6):656–659.
- 975 [23] Chen, J. Y., Wong, K. W., Cheng, L. M., and Shuai, J. W. (2003). A secure communication scheme based on the
976 phase synchronization of chaotic systems. *Chaos*, 13(2):508–514.
- 977 [24] Chen, J. Y., Wong, K. W., Zheng, H. Y., and Shuai, J. W. (2001). Phase signal coupling induced n:m phase
978 synchronization in drive-response oscillators. *Physical Review E*, 63(3):036214 (1–6).
- 979 [25] Chung, F. and Lu, L. (2006). *Complex Graphs and Networks*. American Mathematical Society.
- 980 [26] Cuomo, K. M. and Oppenheim, A. V. (1993a). Chaotic signals and systems for communications. *IEEE*, 4:137–
981 140.
- 982 [27] Cuomo, K. M. and Oppenheim, A. V. (1993b). Circuit Implementation of Synchronized Chaos with Applications
983 to Communications. *Physical Review Letters*, 71(1):65–68.
- 984 [28] Dahms, T., Lehnert, J., and Schöll, E. (2012). Cluster and group synchronization in delay-coupled networks.
985 *Physical Review E*, 86(1):016202 (1–10).
- 986 [29] Dedieu, H., Kennedy, M. P., and Hasler, M. (1993). Chaos shift keying: modulation and demodulation of a
987 chaotic carrier using self-synchronizing Chua’s circuits. *IEEE Trans. Circuits Syst., II: Analog Digital Signal
988 Processing*, 40(10):634–642.
- 989 [30] Dedieu, H. and Ogorzalek, M. J. (1997). Identifiability and identification of chaotic systems based on adaptive
990 synchronization. *IEEE Trans. Circuits Syst., I: Fund. Theory and App*, 44(10):948–962.
- 991 [31] Earn, D. J. D., Levin, S. A., and Rohani, P. (2000). Coherence and Conservation. *Science*, 290(November):1360–
992 1364.
- 993 [32] Earn, D. J. D., Rohani, P., and Grenfell, B. T. (1998). Persistence, chaos and synchrony in ecology and epidemi-
994 ology. *Proc R. Soc. Lond. B*, 265(1390):7–10.
- 995 [33] Eckhardt, B., Ott, E., Strogatz, S. H., Abrams, D. M., and McRobie, A. (2007). Modeling walker synchronization
996 on the millennium bridge. *Physical Review E*, 75(2):021110 (1–10).
- 997 [34] Eldering, J. (2013). *Normally Hyperbolic Invariant Manifolds*. Atlantis Press.
- 998 [35] Fenichel, N. (1972). Persistence and Smoothness of Invariant Manifolds for Flows.
- 999 [36] Fiedler, M. (1973). Algebraic connectivity of graphs. *Czechoslovak Mathematical Journal*, 23(2):298–305.
- 1000 [37] Fu, C., Deng, Z., Huang, L., and Wang, X. (2013). Topological control of synchronous patterns in systems of
1001 networked chaotic oscillators. *Physical Review E*, 87(3):032909 (1–7).
- 1002 [38] Fujisaka, H. and Yamada, T. (1983). Stability Theory of Synchronized Motion in Coupled-Oscillator Systems.
1003 *Progress of Theoretical Physics*, 69(1):32–47.
- 1004 [39] Garcia Dominguez, L., Wennberg, R. A., Gaetz, W., Cheyne, D., Snead, O. C., and Perez Velazquez, J. L. (2005).

- Enhanced synchrony in epileptiform activity? Local versus distant phase synchronization in generalized seizures. *The Journal of Neuroscience*, 25(35):8077–8084.
- [40] Gleick, J. (2011). *Chaos: Making a New Science (Enhanced Edition)*. Open Road Media.
- [41] Golub, G. H. and Van Loan, C. F. (1996). *Matrix Computations*. The Johns Hopkins University Press, third edition.
- [42] Gregoriou, G. G., Gotts, S. J., Zhou, H., and Desimone, R. (2009). High-Frequency, Long-Range Coupling Between Prefrontal and Visual Cortex During Attention. *Science*, 324(5931):1207–1210.
- [43] Grenfell, B. T., Bjørnstad, O. N., and Kappey, J. (2001). Travelling waves and spatial hierarchies in measles epidemics. *Nature*, 414:716–723.
- [44] Hammond, C., Bergman, H., and Brown, P. (2007). Pathological synchronization in Parkinson’s disease: networks, models and treatments. *Trends in Neurosciences*, 30(7):357–364.
- [45] Hart, J. D., Pade, J. P., Pereira, T., Murphy, T. E., and Roy, R. (2015). Adding connections can hinder network synchronization of time-delayed oscillators. *Physical Review E*, 92(2):022804.
- [46] He, R. and Vaidya, P. G. (1992). Analysis and synthesis of synchronous periodic and chaotic systems. *Physical Review A*, 46(12):7387–7392.
- [47] Heagy, J. F., Pecora, L. M., and Carroll, T. L. (1995). Short Wavelength Bifurcations and Size Instabilities in Coupled Oscillator Systems. *Physical Review Letters*, 74(21):4185–4188.
- [48] Hirose, K., Kittaka, S., Oishi, Y., Kannari, F., and Yanagisawa, T. (2013). Phase locking in a Nd:YVO₄ waveguide laser array using Talbot cavity. *Optics Express*, 21(21):24952–24961.
- [49] Hirsch, M., Smale, S., and Devaney, R. (2004). *Differential Equations, Dynamical Systems, and an Introduction to Chaos*. Number v. 60 in Differential equations, dynamical systems, and an introduction to chaos. Academic Press.
- [50] Hodgkin, A. L. and Huxley, A. F. (1952). A quantitative description of membrane current and its application to conduction and excitation in nerve. *J Physiol.*, 117(4):500–544.
- [51] Hramov, A. E. and Koronovskii, A. A. (2004). An approach to chaotic synchronization. *Chaos*, 14(3):603–610.
- [52] Hramov, A. E. and Koronovskii, A. A. (2005). Generalized synchronization: A modified system approach. *Physical Review E*, 71(6):067201 (1–4).
- [53] Huang, L., Chen, Q., Lai, Y. C., and Pecora, L. M. (2009). Generic behavior of master-stability functions in coupled nonlinear dynamical systems. *Physical Review E*, 80:1–11.
- [54] Hunt, B. R., Ott, E., and Yorke, J. A. (1997). Differentiable generalized synchronization of chaos. *Physical Review E*, 55(4):4029–4034.
- [55] Jeffreys, H. and Jeffreys, B. (1988). *Mean-Value Theorems*. Cambridge University Press, 3rd edition.
- [56] Josić, K. and Mar, D. J. (2001). Phase synchronization of chaotic systems with small phase diffusion. *Physical Review E*, 64(5):056234 (1–10).
- [57] Kapitaniak, M., Czolczynski, K., Perlikowski, P., Stefanski, A., and Kapitaniak, T. (2014). Synchronous states of slowly rotating pendula. *Physics Reports*, 541(1):1–44.
- [58] Katok, A. and Hasselblatt, B. (1997). *Introduction to the Modern Theory of Dynamical Systems*. Encyclopedia of Mathematics and its Applications. Cambridge University Press.
- [59] Kocarev, L., Halle, K. S., Eckert, K., Chua, L. O., and Parlitz, U. (1992). Experimental Demonstration of Secure Communications Via Chaotic Synchronization. *International Journal of Bifurcation and Chaos*, 02(03):709–713.
- [60] Kocarev, L. and Parlitz, U. (1995). General Approach for Chaotic Synchronization with Applications to Communication. *Physical Review Letters*, 74(25):5028–5031.
- [61] Kocarev, L. and Parlitz, U. (1996). Generalized Synchronization, Predictability, and Equivalence of Unidirectionally Coupled Dynamical Systems. *Physical Review Letters*, 76(11):1816–1819.
- [62] Kocarev, L., Parlitz, U., and Stojanovski, T. (1996a). An application of synchronized chaotic dynamic arrays. *Physics Letters A*, 217(4-5):280–284.
- [63] Kocarev, L., Parlitz, U., Stojanovski, T., and Panovski, L. (1996b). Generalized synchronization of chaos. *1996 IEEE International Symposium on Circuits and Systems. Circuits and Systems Connecting the World. ISCAS 96*, 3:116–119.
- [64] Kowalski, J. M., Albert, G. L., and Gross, G. W. (1990). Asymptotically synchronous chaotic orbits in systems of excitable elements. *Physical Review A*, 42(10):6260–6263.
- [65] Kuramoto, Y. (1975). Self-Entrainment of a Population of Coupled Non-Linear Oscillators. *Lecture Notes in Physics*, 39(International Symposium on Mathematical Problems in Theoretical Physics):420–423.
- [66] Lorenz, E. N. (1963). Deterministic Nonperiodic Flow. *Journal of the Atmospheric Sciences*, 20(2):130–141.
- [67] Lotrič, M. B. and Stefanovska, A. (2000). Synchronization and modulation in the human cardiorespiratory

- 1060 system. *Physica A*, 283(3):451–461.
- 1061 [68] Lyapunov, A. M. (1992). Stability of motion: general problem. *International Journal of Control*, 55(3):767–772.
- 1062 [69] Maia, D. M., Macau, E. E., and Pereira, T. (2016). Persistence of network synchronization under nonidentical
1063 coupling functions. *SIAM Journal on Applied Dynamical Systems*, 15(3):1563–1580.
- 1064 [70] Masoller, C. (2001). Anticipation in the synchronization of chaotic semiconductor lasers with optical feedback.
1065 *Physical Review Letters*, 86(13):2782–2785.
- 1066 [71] Mohar, B. (1991a). Eigenvalues, diameter, and mean distance in graphs. *Graphs and Combinatorics*, 7(1):53–64.
- 1067 [72] Mohar, B. (1991b). The Laplacian Spectrum of Graphs. *Graph Theory, Combinatorics, and Applications*, Vol.
1068 2, 2:871–898.
- 1069 [73] Mohar, B. (1997). *Some applications of Laplace eigenvalues of graphs*, pages 225–275. Springer Netherlands,
1070 Dordrecht.
- 1071 [74] Motter, A. E., Myers, S. a., Anghel, M., and Nishikawa, T. (2013). Spontaneous synchrony in power-grid
1072 networks. *Nature Physics*, 9(3):191–197.
- 1073 [75] Motter, A. E., Zhou, C., and Kurths, J. (2005a). Network synchronization, diffusion, and the paradox of hetero-
1074 geneity. *Physical Review E*, 71(1):016116 (1–9).
- 1075 [76] Motter, A. E., Zhou, C. S., and Kurths, J. (2005b). Enhancing complex-network synchronization. *Europhysics*
1076 *Letters*, 69(3):334–340.
- 1077 [77] Murphy, T. E., Cohen, A. B., Ravoori, B., Schmitt, K. R. B., Setty, A. V., Sorrentino, F., Williams, C. R. S., Ott,
1078 E., and Roy, R. (2010). Complex dynamics and synchronization of delayed-feedback nonlinear oscillators. *Phil.*
1079 *Trans. R. Soc. A*, 368(1911):343–366.
- 1080 [78] Néda, Z., Ravasz, E., Brechet, Y., Vicsek, T., and Barabási, A.-L. (2000). The sound of many hands clapping.
1081 *Nature*, 403(6772):849–850.
- 1082 [79] Newman, M. E. J. (2003). The Structure and Function of Complex Networks. *SIAM Review*, 45(2):167–256.
- 1083 [80] Newman, M. E. J. (2010). *Networks: An introduction*. Oxford University Press.
- 1084 [81] Nishikawa, T. and Motter, A. E. (2010). Network synchronization landscape reveals compensatory structures,
1085 quantization, and the positive effect of negative interactions. *Proceedings of the National Academy of Sciences of*
1086 *the United States of America*, 107(23):10342–7.
- 1087 [82] Nishikawa, T., Motter, A. E., Lai, Y.-C., and Hoppensteadt, F. C. (2003). Heterogeneity in Oscillator Networks:
1088 Are Smaller Worlds Easier to Synchronize? *Physical Review Letters*, 91(1):014101.
- 1089 [83] Oliva, R. A. and Strogatz, S. H. (2001). Dynamics of a Large Array of Globally Coupled Lasers With Distributed
1090 Frequencies. *International Journal of Bifurcation and Chaos*, 11(09):2359–2374.
- 1091 [84] Oppenheim, A. V., Wornell, G. W., Isabelle, S. H., and Cuomo, K. M. (1992). Signal processing in the context
1092 of chaotic signals. *International Conference on Acoustics, Speech, and Signal Processing, 1992*, 4:117–120.
- 1093 [85] Pade, J. P. and Pereira, T. (2015). Improving Network Structure can lead to Functional Failures. *Scientific*
1094 *reports*, 5:9968.
- 1095 [86] Parlitz, U. (1996). Estimating Model Parameters from Time Series by Autosynchronization. *Physical Review*
1096 *Letters*, 76(8):1232–1235.
- 1097 [87] Parlitz, U., Chua, L. O., Kocarev, L., Halle, K. S., and Shang, A. (1992). Transmission of Digital Signals By
1098 Chaotic Synchronization. *International Journal of Bifurcation and Chaos*, 02(04):973–977.
- 1099 [88] Parlitz, U., Junge, L., and Kocarev, L. (1996). Synchronization-based parameter estimation from time series.
1100 *Physical Review E*, 54(6):6253–6259.
- 1101 [89] Pecora, L. M. and Carroll, T. L. (1990). Synchronization in chaotic systems. *Physical Review Letters*, 64(8):821–
1102 824.
- 1103 [90] Pecora, L. M. and Carroll, T. L. (1991). Driving systems with chaotic signals. *Physical Review A*, 44(4):2374–
1104 2383.
- 1105 [91] Pecora, L. M. and Carroll, T. L. (1998). Master Stability Functions for Synchronized Coupled Systems. *Physical*
1106 *Review Letters*, 80(10):2109–2112.
- 1107 [92] Pecora, L. M. and Carroll, T. L. (2015). Synchronization of chaotic systems. *Chaos: An Interdisciplinary Journal*
1108 *of Nonlinear Science*, 25(9):097611.
- 1109 [93] Pecora, L. M., Sorrentino, F., Hagerstrom, A. M., Murphy, T. E., and Roy, R. (2014). Cluster synchronization
1110 and isolated desynchronization in complex networks with symmetries. *Nature communications*, 5(May):4079.
- 1111 [94] Peng, J. H., Ding, E. J., Ding, M., and Yang, W. (1996). Synchronizing Hyperchaos with a Scalar Transmitted
1112 Signal. *Physical Review Letters*, 76(6):904–907.
- 1113 [95] Pereira, T. (2010). Hub synchronization in scale-free networks. *Physical Review E*, 82(3):036201 (1–4).
- 1114 [96] Pereira, T., Baptista, M., and Kurths, J. (2007a). General framework for phase synchronization through localized

- sets. *Physical Review E*, 75(2):026216.
- [97] Pereira, T., Baptista, M. S., and Kurths, J. (2007b). Phase and average period of chaotic oscillators. *Physics Letters A*, 362(2-3):159–165.
- [98] Pereira, T., Eldering, J., Rasmussen, M., and Veneziani, A. (2014). Towards a general theory for coupling functions allowing persistent synchronization. *Nonlinearity*, 27:501–525.
- [99] Pereira, T., Eroglu, D., Bagci, G. B., Tirnakli, U., and Jensen, H. J. (2013). Connectivity-driven coherence in complex networks. *Physical Review Letters*, 110(23):234103 (1–5).
- [100] Perez, G. and Cerdeira, H. A. (1995). Extracting messages masked by chaos. *Physical Review Letters*, 74(11):1970–1973.
- [101] Pikovsky, A., Rosenblum, M., and Kurths, J. (2001). *Synchronization: A universal concept in nonlinear sciences*. Cambridge University Press, Cambridge.
- [102] Pikovsky, A. S., Rosenblum, M. G., Osipov, G. V., and Kurths, J. (1997). Phase synchronization of chaotic oscillators by external driving. *Physica D*, 104(3-4):219–238.
- [103] Powell, M. J. D. (1964). An efficient method for finding the minimum of a function of several variables without calculating derivatives. *The Computer Journal*, 7(2):155–162.
- [104] Pyragas, K. (1998). Synchronization of coupled time-delay systems: Analytical estimations. *Physical Review E*, 58(3):3067–3071.
- [105] Ren, H.-P., Baptista, M. S., and Grebogi, C. (2013). Wireless communication with chaos. *Physical Review Letters*, 110(18):184101 (1–5).
- [106] Riordan, O. and Selby, A. (2000). The maximum degree of a random graph. *Comb. Probab. Comput.*, 9(6):549–572.
- [107] Rodrigues, F. A., Peron, T. K. D., Ji, P., and Kurths, J. (2016). The Kuramoto model in complex networks. *Physics Reports*, 610:1–98.
- [108] Rosenblum, M. G., Pikovsky, A. S., and Kurths, J. (1996). Phase synchronization of chaotic oscillators. *Physical Review Letters*, 76(3):1804.
- [109] Rosenblum, M. G., Pikovsky, A. S., and Kurths, J. (1997). From Phase to Lag Synchronization in Coupled Chaotic Oscillators. *Physical Review Letters*, 78(22):4193–4196.
- [110] Rulkov, N. F., Sushchik, M. M., Tsimring, L. S., and Abarbanel, H. D. I. (1995). Generalized synchronization of chaos in directionally coupled chaotic systems. *Physical Review E*, 51(2):980–994.
- [111] Sanders, J. A., Verhulst, F., and Murdock, J. (2007). *Averaging Methods in Nonlinear Dynamical Systems*, volume 59. Springer-Verlag New York, second edition.
- [112] Schäfer, C., Rosenblum, M. G., Kurths, J., and Abel, H. H. (1998). Heartbeat synchronized with ventilation. *Nature*, 392(6673):239–240.
- [113] Schultz, P., Peron, T., Eroglu, D., Stemler, T., Ramírez Ávila, G. M., Rodrigues, F. A., and Kurths, J. (2016). Tweaking synchronization by connectivity modifications. *Physical Review E*, 93(6):062211.
- [114] Shiozai, Y., Stefanovska, A., and McClintock, P. V. E. (2010). Nonlinear dynamics of cardiovascular ageing. *Physics Reports*, 488(2-3):51–110.
- [115] Short, K. M. (1994). Step toward unmasking secure communications. *International Journal of Bifurcation and Chaos*, 4(4):959–977.
- [116] Singer, W. (1999). Neuronal Synchrony: A Versatile Code Review for the Definition of Relations. *Neuron*, 24:49–65.
- [117] Sorrentino, F. and Ott, E. (2007). Network synchronization of groups. *Physical Review E*, 76(5):056114 (1–10).
- [118] Sorrentino, F. and Pecora, L. M. (2016). Approximate cluster synchronization in networks with symmetries and parameter mismatches. *Chaos*, 26(9):094823.
- [119] Sparrow, C. (1982). *The Lorenz Equations: Bifurcations, Chaos, and Strange Attractors*. Springer-Verlag New York.
- [120] Stankovski, T., McClintock, P. V. E., and Stefanovska, A. (2014). Coupling functions enable secure communications. *Physical Review X*, 4(1):011026 (1–9).
- [121] Stankovski, T., Ticcinelli, V., McClintock, P. V. E., and Stefanovska, A. (2015). Coupling functions in networks of oscillators. *New Journal of Physics*, 17.
- [122] Stefanovska, A., Lotric, M. B., Strle, S., and Haken, H. (2001). The cardiovascular system as coupled oscillators? *Physiological measurement*, 22(3):535–550.
- [123] Strogatz, S. H. (2003). *Sync: The Emerging Science of Spontaneous Order*. Hyperion.
- [124] Strogatz, S. H., Abrams, D. M., McRobie, A., Eckhardt, B., and Ott, E. (2005). Crowd synchrony on the Millennium Bridge. *Nature*, 438(November):43–44.

- 1170 [125] Stroud, J., Barahona, M., and Pereira, T. (2015). Dynamics of cluster synchronisation in modular networks:
 1171 Implications for structural and functional networks. In *Applications of Chaos and Nonlinear Dynamics in Science*
 1172 *and Engineering-Vol. 4*, pages 107–130. Springer.
- 1173 [126] Sugawara, T., Tachikawa, M., Tsukamoto, T., and Shimizu, T. (1994). Observation of synchronization in laser
 1174 chaos. *Physical Review Letters*, 72(22):3502–3505.
- 1175 [127] Sun, J., Bollt, E. M., and Nishikawa, T. (2009). Master Stability Functions for Coupled Near-Identical Dynam-
 1176 ical Systems. *EPL (Europhysics Letters)*, 60011:11.
- 1177 [128] Tass, P., Rosenblum, M. G., Weule, J., Kurths, J., Pikovsky, A., Volkman, J., Schnitzler, A., and Freund, H.-J.
 1178 (1998). Detection of n:m Phase Locking from Noisy Data: Application to Magnetoencephalography. *Physical*
 1179 *Review Letters*, 81(15):3291–3294.
- 1180 [129] Tönjes, R. (2010). Synchronization transition in the Kuramoto model with colored noise. *Physical Review E*,
 1181 81:055201.
- 1182 [130] Tönjes, R. and Blasius, B. (2009). Perturbation analysis of the Kuramoto phase-diffusion equation subject to
 1183 quenched frequency disorder. *Physical Review E*, 79:016112.
- 1184 [131] Viana, M. (2000). What’s new on lorenz strange attractors? *Math. Intelligencer*, 22(3):6–19.
- 1185 [132] Wiesenfeld, K., Colet, P., and Strogatz, S. H. (1996). Synchronization Transitions in a Disordered Josephson
 1186 Series Array. *Physical Review Letters*, 76(3):404–407.
- 1187 [133] Williams, C. R. S., Murphy, T. E., Roy, R., Sorrentino, F., Dahms, T., and Schöll, E. (2013). Experimen-
 1188 tal observations of group synchrony in a system of chaotic optoelectronic oscillators. *Physical Review Letters*,
 1189 110(6):064104 (1–5).
- 1190 [134] Winfree, A. T. (1967). Biological rhythms and the behavior of populations of coupled oscillators. *Journal of*
 1191 *Theoretical Biology*, 16(1):15–42.
- 1192 [135] Winful, H. G. and Rahman, L. (1990). Synchronized chaos and spatiotemporal chaos in arrays of coupled
 1193 lasers. *Physical Review Letters*, 65(13):1575–1578.
- 1194 [136] Wu, C. W. (2003). Perturbation of coupling matrices and its effect on the synchronizability in arrays of coupled
 1195 chaotic systems. *Physics Letters A*, 319(5-6):495–503.
- 1196 [137] Yamada, T. and Fujisaka, H. (1983). Stability Theory of Synchronized Motion in Coupled-Oscillator Systems.
 1197 II. *Progress of Theoretical Physics*, 70(5):1240–1248.
- 1198 [138] Yamada, T. and Fujisaka, H. (1984). Stability Theory of Synchronized Motion in Coupled-Oscillator Systems.
 1199 III. *Progress of Theoretical Physics*, 72(5):885–894.
- 1200 [139] Yu, D. and Parlitz, U. (2008). Estimating parameters by autosynchronization with dynamics restrictions. *Phys-*
 1201 *ical Review E*, 77(6):066221 (1–7).
- 1202 [140] Zhou, C. and Kurths, J. (2006). Hierarchical synchronization in complex networks with heterogeneous degrees.
 1203 *Chaos*, 16(1):015104 (1–10).
- 1204 [141] Zhou, C., Motter, A. E., and Kurths, J. (2006). Universality in the Synchronization of Weighted Random
 1205 Networks. *Physical Review Letters*, 96(3):034101 (1–4).